Metabolomics study of the synergistic killing of polymyxin B in combination with amikacin against polymyxin-susceptible and -resistant *Pseudomonas aeruginosa*

Maytham Hussein[1,2], Mei-Ling Han[1], Yan Zhu[1], Qi (Tony) Zhou[3], Yu-Wei Lin[1], Robert. E.W. Hancock[4], Daniel Hoyer,[2,5,6] Darren J Creek[7], Jian Li[1*], Tony Velkov[2*]

[1]Monash Biomedicine Discovery Institute, Department of Microbiology, School of Biomedical Sciences, Faculty of Medicine, Nursing and Health Sciences, Monash University, Melbourne, Australia; [2]Department of Pharmacology & Therapeutics, School of Biomedical Sciences, Faculty of Medicine, Dentistry and Health Sciences, The University of Melbourne, Parkville, VIC, 3010, Australia; [3]Department of Industrial and Physical Pharmacy, College of Pharmacy, Purdue University, West Lafayette, IN 47907, USA. [4]Department of Microbiology and Immunology, Centre for Microbial Diseases and Immunity Research, University of British Columbia, Vancouver, British Columbia, Canada; [5]The Florey Institute of Neuroscience and Mental Health, The University of Melbourne, 30 Royal Parade, Parkville, VIC, 3052, Australia; [6]Department of Molecular Medicine, The Scripps Research Institute, 10550 N. Torrey Pines Road, La Jolla, CA 92037, USA; [7]Drug Delivery, Disposition and Dynamics, Monash Institute of Pharmaceutical Sciences, Monash University, Melbourne 3052, Australia.

[†]**Correspondence:** Tony Velkov, Phone: + 61 3 83449846. Fax: +61 3 9903 9583. E-mail: Tony.Velkov@unimelb.edu.au OR Jian.Li@monash.edu

Abstract

In the present study, we employed untargeted metabolomics to investigate the synergistic killing mechanism of polymyxin B in combination with an aminoglycoside, amikacin against a polymyxin-susceptible isolate *P. aeruginosa* FADDI-PA111 (MICs = 2 mg/L for both polymyxin B and amikacin) and a polymyxin-resistant Liverpool Epidemic Strain LESB58 (the corresponding MIC for both polymyxin B and amikacin is 16 mg/L). The metabolites were extracted at 15 min, 1 and 4 h following treatment with polymyxin B alone (2 mg/L for FADDI-PA111; 4 mg/L for LESB58), amikacin alone (2 mg/L) and in combination; and analyzed using LC-MS. At 15 min and 1 h, polymyxin B alone induced significant perturbations in glycerophospholipid and fatty acid metabolism pathways in FADDI-PA111, and to a lesser extent in LESB58. Amikacin alone at 1 and 4 h induced significant perturbations in peptide and amino acid metabolism, which is in line with the mode of action of aminoglycosides. Pathway analysis of FADDI-PA111 revealed that the synergistic effect of the combination was largely due to the inhibition of cell envelope biogenesis which was initially driven by polymyxin B via suppression of key metabolites involved in lipopolysaccharide, peptidoglycan and membrane lipids (15 min and 1 h) and later by amikacin (4 h). Overall, these novel findings demonstrate that the disruption of the cell envelope biogenesis, central carbohydrate metabolism, decreased levels of amino sugars and a downregulated nucleotide pool are the metabolic pathways associated with the synergistic killing of polymyxin-amikacin combination against *P. aeruginosa*. This mechanistic study might help optimizing synergistic polymyxin B combinations in the clinical setting.

Introduction

The World Health Organization (WHO) recently classified multidrug-resistant (MDR) *Pseudomonas aeruginosa* as a top-priority critical pathogen that urgently requires new antibiotic therapies.(1) MDR *P. aeruginosa* often causes life-threatening nosocomial infections such as pneumonia and bloodstream infections, in particular immuno-compromised and critically-ill patients.(2, 3) *P. aeruginosa* is often responsible for the colonization of the lungs in adult cystic fibrosis (CF) patients and is associated with high mortality rates.(4, 5) The large genome (5.9-6.3 Mb) of *P. aeruginosa* encodes complex regulation systems and remarkable metabolic flexibility, endowing it with the ability to rapidly adapt to diverse conditions such as antimicrobial treatment. (6) The known mechanisms of antimicrobial resistance in *P. aeruginosa* include induced efflux pumping, altering target binding sites, and enzymatical inactivation of antibiotics.(7, 8) Most worryingly, *P. aeruginosa* can rapidly develop resistance to all current antibiotics including the last-resort lipopeptide antibiotics, the polymyxins (polymyxin B and colistin, also known as polymyxin E).(9-11)

Polymyxins are non-ribosomal polycationic decapeptides that consist of a cyclic heptapeptide, linked to a tripeptide linear chain and *N*-terminal fatty acyl tail. Polymyxins are amphipathic molecules owing to their five basic L-α-γ -diaminobutyric acid (Dab) residues, two hydrophobic amino acids at position 6 and 7, and the *N*-terminal fatty acyl chain.(12) A model for their mode of action entails that the cationic Dab residues of the polymyxin molecule interact electrostatically with the negatively charged phosphate groups of the lipid A component of lipopolysaccharide (LPS), followed by the displacement of divalent cations (Mg^{2+} and Ca^{2+}) that bridge and stabilize the LPS leaflet of the outer membrane (OM). (13) This then enables the insertion of the *N*-terminal fatty acyl group and the hydrophobic position 6-7 amino acid side chain of the polymyxin into the OM fatty acyl layer, leading to outer membrane destabilization, self-promoted uptake, osmotic imbalance and cell death.

(12, 14) However, there are still significant gaps in the exact mechanism(s) of polymyxin activity and resistance in *P. aeruginosa*.(15) Treatment failure due to suboptimal polymyxin plasma concentrations or the presence of hetero-resistant sub-populations highlights the need to optimize antibiotic combination therapies (e.g. polymyxin B combined with the aminoglycoside amikacin).(16, 17) The most common mechanism of polymyxin resistance in *P. aeruginosa* is mainly related to LPS and involves the addition of phosphoethanolamine (pEtN) and 4-amino-4-deoxy-L-arabinose (L-Ara4N), or by deacylation, hydroxylation and palmitoylation to its lipid A component.(18-20) As a result, the overall net negative charge of the OM is reduced, which attenuates the binding of the polycationic polymyxin molecule.(12) Currently used polymyxin combination therapies are empirical and most combination studies focus only on phenotypical killing.(21) The lack of a fundamental understanding of the mechanistic synergy underlying polymyxin combination therapy hinders their clinical utility. Systems pharmacology is a powerful approach for deciphering the complex interplay between cellular pathways in response to antibiotic treatments(22). Metabolomics is the combination of state-of-the-art bioanalytical techniques and bioinformatics that are of considerable utility for elucidating the complex modes of action and bacterial cellular processes in response to antibiotic killing.(23, 24)

To the best of our knowledge, we are the first to conduct a metabolomics analysis of the synergistic killing mechanism of a polymyxin in combination with amikacin. We profiled the response of the polymyxin-susceptible *P. aeruginosa* (FADDI-PA111) and polymyxin-resistant *P. aeruginosa* (LESB58) following treatment with the polymyxin B-amikacin combination. It was the first to reveal the synergistic bactericidal effect of the combination involves the disruption of bacterial cell envelope biogenesis and inhibition of the central carbohydrate metabolism and the pyridine nucleotide cycle.

Results

Metabolic impact of polymyxin B, amikacin and their combination on polymyxin-susceptible P. aeruginosa FADDI-PA111

Lipopolysaccharides biosynthesis, pyridine nucleotide cycle, central carbon metabolism and peptidoglycan biosynthesis are the main influenced pathways due to polymyxin B and amikacin monotherapies and their combination.

Lipid metabolism. Lipid levels were markedly perturbed in *P. aeruginosa* FADDI-PA111 following polymyxin B monotherapy and the combination at 15 min, 1 and 4 h. Polymyxin B treatment predominantly perturbed bacterial membrane lipids across all time points, including fatty acids (FAs) and glycerophospholipids (GPLs) ($\geq$ 0.58553-$\log_2$-fold, $p \leq 0.05$, false discovery rate [FDR] $\leq$ 0.1) (**Figure 1A**). The impact of amikacin on the levels of these lipid metabolites at 15 min was marginal; however, amikacin induced significant perturbations of lipid levels at 1 h and 4 h. Intriguingly, the combination produced a differential pattern of lipid perturbation across all three-time points, notably more GPLs perturbations were evident than FAs (**Figures 1A and 1B**). The combination significantly reduced the concentration of palmitoleyl-CoA ($\geq$ -2.0-$\log_2$-fold, $p \leq 0.05$, FDR $\leq$ 0.05), across all three time points (**Figure 1B**).(25) Furthermore, a key precursor of membrane phospholipids, *sn*-glycerol 3-phosphate, was significantly decreased following the combination treatment at 15 min and 1 h ($\geq$ -1.0-$\log_2$-fold, $p \leq 0.05$, FDR $\leq$ 0.05). The levels of essential bacterial membrane lipids involved in phospholipid and LPS biosynthesis were significantly reduced following the combination treatment, including *sn*-glycero-3-phosphoethanolamine, FA hydroxy (14:0) (3-hydroxymyristic acid) and FA (14:1) (myristoleic acid) ($\geq$ -1.0-$\log_2$-fold, $p \leq 0.05$, FDR $\leq$ 0.05) (**Figures 1A&1B**). Our results suggest that the combination of polymyxin B and

amikacin reduced the main precursors of bacterial membrane lipids, particularly those related to LPS and GPL biosynthesis.

LPS biosynthesis. As alluded to above, the combination treatment substantially decreased the levels of intermediates involved in LPS biosynthesis, particularly at 1 h . At 15 min, the polymyxin-amikacin combination caused a prominent decline in the concentrations of three essential pentose phosphate pathway (PPP) metabolites (≥ -2.0-$\log_2$-fold, $p \leq 0.05$, FDR ≤ 0.05), namely D-ribose 5-phosphate, erythrose 4-phosphate and D-sedoheptulose-7-phosphate. The levels of three precursors of LPS biosynthesis underwent a remarkable decreased (≥ -2.0-$\log_2$-fold, $p \leq 0.05$, FDR ≤ 0.05) after combination treatment at 15 min, including ADP-D-glycero-D-manno-heptose, 3-deoxy-D-manno-octulosonate (KDO) and UDP-*N*-acetyl-D-glucosamine (UDP-Glc-NAc) (**Figure 2A**). Polymyxin B monotherapy had a similar impact on LPS biosynthesis wherein four key metabolites underwent a significant decline (≥ -1.0-$\log_2$-fold, $p \leq 0.05$, FDR ≤ 0.05), including D-sedoheptulose 7-phosphate, ADP-D-glycero-D-manno-heptose, 3-deoxy-D-manno-octulosonate (KDO) and UDP-Glc-NAc (**Figure 2A**). On the other hand, the effect of amikacin treatment on the FADDI-PA111 LPS biosynthetic pathway was unremarkable. Interestingly, the combination at 1 h induced a significant decrease (≥ -1.0-$\log_2$-fold, $p \leq 0.05$, FDR ≤ 0.05) in the levels of seven metabolites that are crucial for the formation of LPS, namely D-ribose 5-phosphate, D-sedoheptulose 7-phosphate, CMP-KDO, KDO, UDP-Glc-NAc, ADP-D-glycero-D-manno-heptose, and D-glycero-D-manno-heptose 1,7-bisphosphate (**Figure 2B (i&ii)**). Similarly, to a lesser extent, polymyxin B monotherapy induced a significant drop in the levels of three key intermediates of the LPS biosynthetic pathway, including UDP-Glc-NAc, KDO and ADP-D-glycero-β-D-manno-heptose. Similar to the 15 min time point, we did not observe any impact on the LPS biosynthesis at 1 h following amikacin monotherapy (**Figure 2B (ii)**). The combination also induced a significant decrease (≥ -1.0-$\log_2$-fold, $p \leq 0.05$, FDR ≤ 0.05) in

the levels of key precursors of LPS biogenesis at 4 h, namely ADP-D-glycero-D-manno-heptose, KDO, UDP-Glc-NAc and D-glycero-D-manno-heptose 1,7-bisphosphate (**Figure 2C**). Amikacin monotherapy reduced the levels of four key intermediates of LPS biosynthesis, namely ADP-D-glycero-D-manno-heptose, D-glycero-D-manno-heptose 1,7-bisphosphate, KDO, and UDP-Glc-NAc at 4 h (≥ -1.0-$\log_2$-fold, $p \leq 0.05$, FDR ≤ 0.05) (**Figure 2C**). On the other hand, the influence of polymyxin B monotherapy on LPS biosynthesis in FADDI-PA111 at 4 h was unremarkable.

Central carbon metabolites. Besides the significant impact of the polymyxin B-amikacin combination on pentose phosphate pathway (PPP) of FADDI-PA111 at 15 min and 1 h, it also caused a remarkable suppression in the levels of five key intermediates of the glycolysis pathway at 1 h, including glycerate-3-phosphate, D-fructose-6-phosphate, D-glucose-6-phosphate, glyceraldehyde-3-phosphate and phosphoenolpyruvate (≥ -1.0-$\log_2$-fold, $p \leq 0.05$, FDR ≤ 0.05) (**Figures 3A and 3B**). Moreover, the combination significantly reduced the concentrations of eight TCA cycle metabolites, namely acetyl-CoA, citrate, *cis*-aconitate, isocitrate, succinate, fumarate, NAD^+ and CoA (≥ -1.0-$\log_2$-fold, $p \leq 0.05$, FDR ≤ 0.05) (**Figures 3A&B**). Polymyxin treatment only induced a significant reduction in the concentrations of two intermediates of this pathway at 1 h, namely succinate ($\log_2$ fold change = -1.13) and CoA ($\log_2$ fold change = -1.48); amikacin monotherapy had no detectable impact on the central carbon metabolites at 1 h (**Figure 3B**).

Pyridine nucleotide cycle. Treatment with polymyxin B alone and the combination (**Figure 4A**) markedly disrupted the pyridine nucleotide cycle PNC pathway particularly at 15 min and to a lesser extent at 1 h (≥ 1.0-$\log_2$-fold, $p \leq 0.05$, FDR ≤ 0.05). Polymyxin B treatment decreased the levels of two key metabolites, namely nicotinamide and $NADP^+$ at 15 min. Whereas, the combination reduced the levels of six key metabolites compromising the backbone of the PNC, namely iminoaspartate, nicotinamide, $NADP^+$, NAD, ATP and

glycerone phosphate at 15 min (**Figure 4B (i)**). At 1 h, the combination reduced the levels of four metabolites, namely iminoaspartate, $NADP^+$, NAD and glycerone phosphate (**Figure 4B (ii)**). The influence of amikacin monotherapy on the PNC was inconsequential across all time points. Based on these findings we purport that the perturbations in PNC metabolites by the combination were largely driven by polymyxin B.

Nucleotide levels. Polymyxin B monotherapy induced a marked decline in the levels of nucleotides across all the time points, and this effect was even more pronounced following combination treatment (≥1.0-$\log_2$-fold, p ≤0.05, FDR≤0.1) (**Figures 5A&B, Supplementary Table 2**). At 15 min, a marked decline in the levels of five nucleotides (hypoxanthine, xanthine, dTMP, dCMP and dTDP) was observed following polymyxin B monotherapy, whereas amikacin monotherapy had negligible effects. Nine nucleotides underwent a remarkable decrease in their levels after combination treatment (except for an increment in orotate levels) (**Figure 5A (i)**). At 1 h, the combination profoundly reduced (≥ -1.0-$\log_2$-fold, p ≤0.05, FDR ≤0.05) the concentrations of 16 nucleotide intermediates (**Figure 5B , Supplementary Table 2**). Similarly, to the 15 min time point, polymyxin B monotherapy caused a reduction of six nucleotides and conversely induced an increase in the levels of orotate (≥1.0-$\log_2$-fold, p ≤ 0.05, FDR ≤ 0.1). Amikacin monotherapy increased (≥1.0-$\log_2$-fold, p ≤ 0.05, FDR ≤ 0.1) the concentrations of 5-phosphoribosylamine at 1 h (**Figure 5A (ii)**). Key nucleotides were also significantly depleted in FADDI-PA111 following the combination treatment at 4 h (**Figure 5B**).

Amino acid, peptide and peptidoglycan metabolism. Differential perturbation patterns in amino acid metabolism were identified following each treatment condition across all time points; the most notable difference was evident in the main precursors of peptidoglycan

biosynthesis and arginine metabolism (**Figure 6**). A dramatic decrease in the levels of four essential metabolites of the peptidoglycan biosynthetic pathway was observed following polymyxin B monotherapy at 15 min (≥ -1.5-$\log_2$-fold; $p \leq 0.05$; FDR ≤0.05), including D-alanyl-D-alanine, UDP-*N*-acetylmuramoyl-L-alanyl-D- γ-glutamyl-*meso*-2,6-diaminopimelate (UDP-MurNAc-L-Ala- γ-D-Glu-m-DAP), UDP-*N*-acetylmuramate (UDP-MurNAc) and *N*-acetyl-D-glucosamine-6-phosphate (**Figure 6A (i,ii)**). This effect was less pronounced at the latter time points of 1 and 4 h (**Figure 6B and 6C**). Amikacin monotherapy caused a moderate increase (≥ 0.58553-$\log_2$-fold, $p \leq 0.05$, FDR ≤ 0.1) in the levels of four intermediates of histidine metabolism at 15 min (except for a decline in imidazole-4-acetate levels), namely imidazol-5-yl-pyruvate, *N*-formimino-L-glutamate and urocanate (**Figure 6A(i)**). On the other hand, the combination treatment resulted in a significant suppression of the levels of key intermediates of peptidoglycan biosynthesis at 15 min, including D-alanyl-D-alanine, UDP-MurNAc-L-Ala-γ-D-Glu-m-DAP, UDP-MurNAc and *N*-acetyl-D-glucosamine 6-phosphate (≥ -2.0-$\log_2$-fold, $p \leq 0.05$, FDR ≤ 0.05) (**Figures 6A (i,ii)**). This effect on peptidoglycan biosynthesis persisted over the latter time points; in particular at 1 h, causing a dramatic decrease in the levels of five metabolites D-alanyl-D-alanine, Alanine, UDP-MurNAc-L-Ala-γ-D-Glu-m-DAP, UDP-*N*-acetylmuramate (UDP-MurNAc) and *N*-acetyl-D-glucosamine 6-phosphate (≥ -1.0-$\log_2$-fold, $p \leq 0.05$, FDR ≤ 0.05) (**Figure 6B(i,ii)**). This effect tapered at 4 h at which the combination therapy reduced the concentrations of only two important intermediates of peptidoglycan biosynthesis namely alanine ($\log_2$ fold change = -2.02) and *N*-Acetyl-D-glucosamine 6-phosphate ($\log_2$ fold change = -1.26) (**Figure 6C**). The effect of the polymyxin-amikacin combination on the intermediates of arginine metabolism was most pronounced at 15 min and 1 h, reducing the levels of N_2-succinyl-L-ornithine and *N*-acetyl-L-glutamate (at 15 min) and of *N*-acetyl-L-glutamate, L-1-pyrroline-3-hydroxy-5-carboxylate, L-glutamine and *N2*-succinyl-L-arginine

(at 1 h) (**Figures 6A and 6B (i, iii)**). Amikacin treatment and the combination induced major perturbations in peptides. The combination treatment significantly decreased the levels of two essential peptides glutathione and L-Ala-D-Glu-*meso*-A2pm-D-Ala (muropeptide) at 15 min ($\geq$ -1.0-$\log_2$-fold, $p \leq 0.05$, FDR ≤ 0.05) (**Figure 7A**). Twelve peptide metabolites (including glutathione; $\geq$ -2.0-$\log_2$-fold, $p \leq 0.05$, FDR ≤ 0.05) were remarkably diminished after 1 h of the combination treatment (**Figure 7B**). The combination treatment produced a marginal effect on peptide metabolism at 4 h (**Figure 7C**). Amikacin monotherapy increased the levels of six peptide metabolites at 15 min and then induced a significant reduction in their levels at 1 and 4 h (**Figures 7A-C**). Polymyxin B monotherapy did not show a significant impact on peptide metabolism across all time points except for 1 h (**Figure 7B**). Furthermore, a glutathione level underwent a significant decline after polymyxin B treatment at 15 min and 1 h ($\geq$ -2.0-log2-fold, p $\leq$ 0.05, FDR $\leq$ 0.05). It should be noted that peptide identifications were based on accurate mass and isomeric forms of the putative peptides where possible.

Impact of polymyxin B, amikacin, and their combination on the metabolome of the polymyxin-resistant CF P. aeruginosa isolate LESB58

The Liverpool epidemic strain LESB58 is intrinsically resistant to polymyxin B and amikacin as its resistome carries aminoglycoside resistance genes APH(3′′)-IIb which mediate the inactivation of amikacin via aminoglycoside-modifying enzyme (phosphotransferase).(18, 26) Not surprisingly, the metabolic response of the strain was limited to all treatment conditions except for minor effects on lipid and carbohydrate metabolism; the only significantly perturbed metabolites were comparable in number between polymyxin B monotherapy and combination treatment groups across all time points (**Supplementary Figure S4B**). Polymyxin B monotherapy caused a marked reduction in the levels of metabolites from amino acid, lipid, and carbohydrate metabolism at 15 min and 1 h,

242 including amino acid intermediates involved in glutathione metabolism such as glutathione
243 disulfide (log_2 fold change = -2.07), L-glutamate (log_2 fold change = -1.14), and *s*-
244 glutathionyl-L-cysteine (log_2 fold change = -1.44) (**Supplementary Figure S6B**;
245 **Supplementary Table 3**). Palmitoleyl-CoA (log_2 fold change = -0.82) and oleoyl-CoA (log_2
246 fold change= -0.82) were among essential lipid membrane intermediates that underwent a
247 marked decline following polymyxin B monotherapy. However, the effect of polymyxin B
248 monotherapy was completely inversed at 4 h wherein the levels of all intermediates
249 increased. On the other hand, amikacin treatment showed a delayed effect wherein marginal
250 perturbation was evident at 15 min, followed by dramatic changes at 1 and 4 h
251 (**Supplementary Figures S4B&S6B**); amikacin monotherapy imparted a significant
252 perturbation (≥1.0-log_2-fold, $p \leq 0.05$, FDR ≤ 0.05) in the levels of glutathione biosynthesis
253 related intermediates such as glutathione disulfide, L-methionine *S*-oxide, L-methionine and
254 *O*-acetyl-L-homoserine (**Supplementary Table 3**).

255 The polymyxin B-amikacin combination treatment mainly caused perturbation to
256 lipids, which were primarily decreased at 15 min and 1 h; while increases were generally
257 observed at 4 h. The main lipid precursors involved in the bacterial outer membrane
258 composition underwent a remarkable perturbation following the combination treatment (≥1.0-
259 log_2-fold, $p \leq 0.05$, FDR ≤ 0.05), namely FA (16:0), FA (17:0), FA (18:0), FA (14:1) and *sn*-
260 glycero-3-phosphoethanolamine (log_2 fold change= -0.90) (**Supplementary Table 3**). In
261 addition, carbohydrates were also significantly perturbed. There was an elevation in the levels
262 of intermediates (UDP-L-Ara4FN) associated with the lipid A aminoarabinose modification
263 pathway following polymyxin B monotherapy (15 min and 4 h); however, this effect was not
264 observed with the combination treatment at any time points (**Supplementary Table 3**).

265

Discussion

In the present study, we employed metabolomics to characterise the responses of *P. aeruginosa* to the treatment with polymyxin-amikacin. Polymyxins and aminoglycosides exert their primary antibacterial killing activity via disruption of the OM and inhibition of protein synthesis, respectively.(12, 27) To the best of our knowledge, this is the first study to investigate the antibacterial killing synergy of the combination of polymyxin B with amikacin using an untargeted metabolomics approach. The most significant findings of the study include: (1) differential time-dependent inhibition of key metabolic pathways; (2) perturbation of central carbon metabolism and suppression of nucleotide pools; (3) inhibition of the pyridine nucleotide cycle (the main pool of NADP); and (4) inhibition of LPS and cell wall biosynthesis.

The early cellular metabolic perturbations following treatment with polymyxin B monotherapy seen at 15 min and 1 h impacted lipid, nucleotide, amino- nucleotide-sugars and energy metabolism. Similar metabolic changes were evident following amikacin monotherapy (particularly LPS biosynthesis), albeit in a delayed fashion, largely occurring 4 h post-treatment. Moreover, amikacin monotherapy induced substantial perturbations in peptide metabolism; whereas polymyxin B had little effect on peptide levels (**Supplementary Figure S6A**). These mechanistic findings support the use of the polymyxin B and amikacin combination for maintaining a persistent antibacterial effect (i.e. polymyxin B early and rapid onset, followed by amikacin delayed onset bacterial killing) and minimizing potential bacterial regrowth which can rapidly emerge with monotherapy.(28, 29)

It has been shown that the disorganizing of the bacterial outer membrane is one of the possible bacterial killing mechanism caused by polymyxins.(12, 30) Coincidently, treatment of FADDI-PA111 with polymyxin B monotherapy caused marked suppression of several key phospholipids, fatty acids and lipid intermediates such as FA (16:0), FA (14:1), oleoyl-CoA, and palmitoleylCoA at 15 min, and to a lesser extent at 1 h and 4 h (**Figure 1 A and 3B**). This finding is in agreement with the previous metabolomics studies with *P. aeruginosa* that revealed that polymyxin B caused perturbations in fatty acids and glycerophospholipids.(31, 32) Additionally, it has been found that the genes associated with bacterial OM biosynthesis were differentially expressed as a result of colistin treatment.(33) Membrane fatty acid composition and fluidity are vital for the development of antibiotic resistance, (34, 35) and an increase in saturated fatty acids is usually associated with a decrease in the membrane fluidity and hence, gives rise to a less permeable bacterial OM.(36) It is not surprising that polymyxin B did not show marked perturbations in the lipid intermediates of polymyxin-resistant LESB58 at 15 min; however, a minor reduction in the levels of essential bacterial membrane lipids was evident at 1 h, which was then followed by a significant rise in all significantly affected lipid intermediates at 4 h. These results are likely reflective of the resistance of this strain to polymyxin B.

Amikacin is semi-synthetic aminoglycoside which exerts its bacterial killing activity by interfering with intracellular protein synthesis.(37) However, several studies have shown that aminoglycoside-based amphiphiles (like amikacin-, and neamine-based amphiphiles) are able to disrupt the negatively charged lipids from bacterial inner membranes in *P. aeruginosa*, which subsequently leads to membrane permeabilization and depolarization.(38, 39) Interestingly, our results are in line with these studies as amikacin remarkably reduced the levels of several membrane glycerophospholipids in FADDI-PA111, such as PS (36:0) and PS (37:0) at 4 h (**Figure 1A(iii)**). These glycerophospholipids are commonly involved in

the biosynthesis of phosphatidic acid (PA), the key intermediate in the synthesis of all membrane glycerolipids.(40) The biogenesis of bacterial OM phospholipids starts via acylation of *sn*-glycerol-3-phosphate using fatty acyl-acyl carrier protein (acyl-ACP).(25) Importantly, a previous study has shown that the decline in the levels of palmitoleyl-CoA could lead to decreases in the stability of LpxC, which has a vital role in lipid A core formation.(25) It is important to note that the combination treatment remained effective in reducing the levels of FADDI-PA111 membrane lipids at 4 h in which more perturbations in glycerophospholipids metabolism were most prominent (**Figure 1A(iii)**). In regard to LESB58, the impact of combination treatment was largely related to changes in the levels of fatty acids and glycerophospholipids over 4 h (**Supplementary Table 3**). Together, the above data highlight that the perturbation of lipid metabolism is a key pathway in killing synergy by the polymyxin B and amikacin combination.

Importantly, our study is the first to report that combining polymyxin B with amikacin caused a significant suppression of intermediates involved in LPS biosynthesis (**Figure 2A-C**). This influence may have arisen from the early (15 min and 1 h) inhibition of pentose phosphate pathway (PPP) which is a key source of precursors for LPS synthesis. A considerable decline in intermediates of LPS formation was observed after polymyxin B monotherapy at 15 min and 1 h, but not at 4 h (**Figure 2C**). In contrast, amikacin had no impact at early time points (15 min and 1 h), while it caused substantial inhibitory effects on LPS biosynthesis at 4 h. The combination effect on these pathways was not seen in the polymyxin B resistant strain LESB58; however, the PPP metabolite D-sedoheptulose 7-phosphate was slightly decreased after polymyxin B monotherapy at 15 min (**Supplementary Table 3**). This negative impact on LPS biosynthesis is in line with the primary mode of action of polymyxins that involves disorganising the bacterial OM through its interaction with LPS.(41) It was previously shown that *E. coli* mutants defective in the biosynthesis of

KDO are extremely susceptible to very low concentrations of antibiotics such as novobiocin,(42) and others also noticed that inactivation of D-arabinose-5-phosphate isomerase (API), an enzyme that promotes the reversible isomerization of D-ribulose-5-phosphate (Ru5P) to D-arabinose-5-phosphate, a KDO precursor in *E. coli*, resulted in death of the microorganism.(43) Heptose units such as D-sedoheptulose 7-phosphate are crucial building blocks that form the LPS inner core of Gram-negative bacteria.(44) Heptose-deficient *Haemophilus influenza* mutants, bearing a genetic defect of ADP-glyceromannoheptose isomerase, showed less virulency and more susceptibility to antibiotics.(45) Hence, taking all of the aforementioned studies together, a possible mechanism of synergistic killing by the polymyxin B and amikacin combination is strongly related to the inhibition of PPP and subsequent LPS biosynthesis; and the differential time-dependent inhibition of this pathway by each antibiotic alone is beneficial in terms of PK/PD, due to maintaining of their killing activity over time.

Apart from its potential impact on membrane structure, our pathway analysis illustrated that polymyxin B - amikacin combination also effectively perturbed the TCA and glycolysis (central carbohydrate metabolism) pathways in FADDI-PA111 (**Figures 3A and 3B**). This effect was not evident for LESB58, only two intermediates (succinate and CoA) from these pathways were affected by polymyxin B monotherapy, with no effect seen for amikacin monotherapy. Bacterial central carbohydrate metabolism is a complex cellular network including various metabolic pathways such as glycolysis and TCA, and has been recently investigated as a new target for the next generation of antibiotics.(46) Glycolysis is the main source of acetyl-CoA, which has a direct role in many metabolic processes such as supply of acetyl groups to TCA, synthesis of fatty acids, and amino acid biosynthesis.(47) The TCA cycle has a crucial role in cellular respiration of bacteria and supplies several important intermediates, such as succinate and citrate, which are required for other key

metabolic processes.(48) It is important to mention that there are two fundamental types of reactions that control the TCA cycle, namely anaplerotic and cataplerotic reactions in which the amount of TCA cycle intermediates increases or decreases, respectively.(49) Our results demonstrated that polymyxin B-amikacin treatment displayed a cataplerotic effect on TCA cycle by reduction of fundamental intermediates such as succinate and acetyl-CoA which are essential for electron transport chain reactions, fatty acid and amino acid metabolism.

The polymyxin B - amikacin combination also caused a dramatic perturbation in the pyridine nucleotide cycle (PNC) of FADDI-PA111, with a greater effect seen at 15 min and to a lesser extent at 1 h (**Figures 4A and 4B**). In contrast, polymyxin B monotherapy was only able to reduce the concentrations of two essential precursors of PNC at 15 min, namely nicotinamide and $NADP^+$ (**Figures 4A and 4B (i)**), whilst no effect was seen for amikacin monotherapy. The PNC is an essential network of biochemical transformations that enable bacterial cells to maintain the homeostasis of NADP.(50) It has been found that a small change in the concentration of NADP is likely associated with propagation of various metabolic disruptions, for instance, in the synthesis of proteins and lipids.(51) Inhibition of PNC by polymyxin B-amikacin treatment appears to be a mechanism underlying the synergistic killing activity of the combination.

Polymyxin B-amikacin combination treatment caused a significant reduction in D-ribose-5-phosphate, a key initial intermediate in purine and pyrimidine metabolism and concomitantly produced a significant depletion in the nucleotide pool of FADDI-PA111 up to 4 h. It was evident that the maximum effect on the nucleotide pool was at 1 h followed by 4 h. Similarly, polymyxin B monotherapy demonstrated significant perturbations in the nucleotide levels, especially those related to purine catabolism such as hypoxanthine and xanthine at 15 min and 1 h, which then faded away at 4 h (**Figure 5A&B**). Amikacin had little impact on the nucleotide pool compared to polymyxin B monotherapy and the

389 combination. No significant effect on nucleotide levels was seen in LESB58. Previous
390 metabolomics studies showed that exposure of Gram-negative (*E. coli*) and Gram-positive
391 (*Staphylococcus aureus*) bacteria to different antibiotic treatments (e.g. ampicillin,
392 kanamycin, norfloxacin, and vancomycin) can lead to a depletion of the nucleotide pool,
393 indicative of nucleotide degradation.(52, 53)

394 Notably, the polymyxin B - amikacin combination caused significant inhibition in
395 peptidoglycan biosynthesis only in FADDI-PA111 (**Figure 6A-C**). Levels of major
396 metabolites of peptidoglycan biogenesis were dramatically decreased following the
397 combination treatment across all time points, in particular at 1 h (**Figure 6B(ii)**).(54) This
398 effect might be secondary to the marked depletion of amino- and nucleotide-sugar
399 intermediates that supply key precursors for peptidoglycan biosynthesis.(55) Polymyxin B
400 monotherapy also produced a significant depletion of peptidoglycan intermediates in FADDI-
401 PA111 at 15 min (**Figure 6A**), while there was no noticeable impact following amikacin
402 monotherapy. Interestingly, our group had previously reported transcriptomics and
403 metabolomics studies demonstrating that polymyxins also inhibit peptidoglycan biosynthesis
404 in *A. baumannii and P. aeruginosa* .(32, 56, 57) Pathway analysis highlighted the significant
405 impact of the combination on arginine and proline metabolism in FADDI-PA111 at 15 min
406 and 1 h; and there was a little influence by polymyxin B and amikacin monotherapy on this
407 pathway at 1 and 4 h, respectively (**Figures 6A-C**). The disruption of amino acid pathways,
408 in particular arginine metabolism, has recently been targeted as a novel approach to manage
409 bacterial infections and subvert pathogenesis.(58)

410 Overall, this study highlights the importance of elucidating the complex and dynamic
411 interaction of multiple cellular metabolic pathways due to antibiotic treatment, which
412 ultimately aids in optimizing the most commonly used combination therapy in clinical
413 practice.

414

415

Materials and Methods

Drugs and bacterial isolates

Polymyxin B (Beta Pharma, China, Batch number 20120204) and amikacin (Sigma-Aldrich, Saint Louis, USA) solutions were prepared in Milli-Q™ water (Millipore, Australia) and filtered through 0.22-µm syringe filters (Sartorius, Australia). All other reagents were purchased from Sigma-Aldrich (Australia) and were of the highest commercial grade available. A polymyxin-susceptible *P. aeruginosa* FADDI-PA111 (polymyxin B MIC = 2 mg/L; amikacin MIC = 2 mg/L) and the polymyxin-resistant cystic fibrosis *P. aeruginosa* isolate LESB58 (Liverpool Epidemic strain, MIC = 16 mg/L for both polymyxin B and amikacin) were tested. The isolates were stored in tryptone soy broth (Oxoid) with 20% glycerol (Ajax Finechem, Seven Hills, NSW, Australia) in cryovials at -80°C. Before use, both strains (FADDI-PA111 & LESB58) were sub-cultured onto M9 minimal media (Cold Spring Harbor Protocol 2016).(59)

Bacterial culture preparation for metabolomics experiments

To investigate the possible molecular mechanisms of polymyxin B and amikacin combination, we employed untargeted metabolomics to determine the changes in different metabolite levels following 15 min, 1 and 4 h of antibiotic.

A single colony of *P. aeruginosa* grown on nutrient or Mueller-Hinton agar were opted and grown overnight (16 - 18 h) in 20 mL in M9 minimal media (Cold Spring Harbor Protocol 2016)(59) in 50 mL Falcon tubes (Thermo Fisher, Australia) incubated in a shaking water bath at 37°C (shaking speed, 180 rpm). *P. aeruginosa* LES isolates are methionine auxotrophs; therefore, L-methionine was added to M9 minimal media for growing of the LESB58 strain. Following overnight incubation, each culture was transferred to a 1-L conical flask with 250 mL of fresh M9 minimal media at ~50-100-fold dilutions. Flasks were

incubated at 37°C with shaking at 180 rpm for ~3 - 4 h to log-phase (OD_{600} ~0.5). Cultures (50 mL) were transferred to four 500 mL conical flasks and solutions of polymyxin B, amikacin, or both added to three of four flasks to give a final concentration of 2 mg/L for FADDI-PA111; 4 mg/L for LESB58 for polymyxin B and 2 mg/L for amikacin for both strains; the remaining flask acted as a drug-free control. To prevent excessive bacterial killing, preliminary optimization studies were conducted using high bacterial inoculum size (~10^8 cfu/mL) and different antibiotics concentrations to ensure no more than 2-log10 (CFU/mL) reduction and thereby, induce more stress on microorganism. The flasks were further incubated at 37°C with shaking at 180 rpm. After 2 h, the OD_{600} reading for each flask was measured and normalized to ~0.5 with fresh M9 minimal media and 10 mL samples transferred to 15 mL Falcon tubes (Thermo Fisher, Australia) for metabolite extraction. To account for inherent random variation, four biological samples were prepared for each treatment condition for each strain.

Metabolite extraction for metabolomic studies

Following bacterial culture preparation, extraction of metabolites was immediately carried out in order to decrease further drug effects on metabolite levels. Initially, samples were centrifuged at 3220 × *g* at 4˚C for 20 min. Supernatants were then removed and bacterial pellets washed twice in 1 mL of cold normal saline followed by centrifugation at 3220 × *g* at 4˚C for 10 min to remove residual extracellular metabolites and medium components. Then, a 300 µl of cold chloroform:methanol:water (CMW; 1:3:1, v/v) extraction solvent containing 1 µM each of the internal standards (CHAPS, CAPS, PIPES and TRIS) was added to the washed pellets. The used internal standards are physicochemically different small molecules not naturally exist in any microorganism. Samples were then thrice immersed in liquid nitrogen, thawed on ice and vortexed to liberate the intracellular metabolites. The samples were centrifuged for 10 min at 3220 × *g* at 4˚C after third freeze-thaw cycle, whereby 300 µL

of the supernatants was taken to 1.5 mL Eppendorf tubes. Centrifugation at 14,000 × *g* at 4˚C for 10 min was used to detach any particles from samples, and 200 µL transferred into the injection vials for storage in -80 freezer. For LC-MS analysis (described below), the samples were taken out from -80 freezer to thaw and 10 µL of each sample was transferred to vial and used as a pooled quality control sample (QC); namely, a sample that contains all the analytes that will be encountered during the analysis.(60)

LC-MS analysis

Metabolites were identified with hydrophilic interaction liquid chromatography (HILIC) - high-resolution mass spectrometry (HMS) using a Dionex high-performance liquid chromatography (HPLC) system (RSLC U3000, Thermo Fisher) with a ZIC-pHILIC column (5 µm, polymeric, 150 × 4.6 mm; SeQuant, Merck). The system was coupled to a Q-Exactive Orbitrap mass spectrometer (Thermo Fisher) operated in both positive and negative electro-spray ionization (ESI) mode (rapid switching) at 35,000 resolution with a detection range of 85 to 1, 275 m/z. Two LC solvents (A) 20 mM ammonium carbonate and (B) acetonitrile were used, which operated via a multi-step gradient system. The gradient started at 80% B which declined to 50% B over 15 min and then reduced from 50% B to 5% B over 3 min, followed by wash with 5% B for another 3 min, and finally 8 min re-equilibration with 80% B at a flow rate of 0.3 mL/min.(61) The injection sample volume was 10 µL and the total run time was 32 min. All samples were analyzed as a single LC-MS batch to avoid batch-to-batch variation. Mixtures of pure standards containing over 300 metabolites were also included in the analysis batch to aid metabolite identification.

Data processing, bioinformatics and statistical analyses

Conversion of LC-MS raw data to metabolite levels was conducted using IDEOM (http://mzmatch.sourceforge.net/ideom.php) software,(62) which initially employed ProteoWizard to convert raw LC-MS data to mzXML format and XCMS to pick peaks with Mzmatch.R to convert to peakML files.(63, 64) Mzmatch.R was subsequently used for the alignment of samples and the filtering of peaks using a minimum peak intensity threshold of 100,000, relative standard deviation (RSD) of < 0.5 (reproducibility), and peak shape (codadw) of > 0.8. Mzmatch was also used to retrieve missing peaks and annotate of related peaks. Default IDEOM parameters were used to eliminate unwanted noise and artifact peaks. Loss or gain of a proton was corrected in negative and positive ESI mode, respectively, followed by putative identification of metabolites by the exact mass within 2 ppm. Retention times of authentic standards were used to confirm the identification of each metabolite (Level 1 identification based on MSI standards). Other metabolites were putatively identified (Level 2 identification based on MSI standards) using exact mass and predicted retention time based on the Kyoto Encyclopedia of Genes and Genomes (KEGG), MetaCyc, and LIPIDMAPS databases, using preference to bacterial metabolites annotated in EcoCyc in cases where isomers could not be clearly differentiated by retention time. Raw peak intensity was used to quantify each metabolite. The free online tool MetaboAnalyst 3.0 was used for the statistical analysis. Briefly, putative metabolites with median RSD ≤ 0.2 (20%) within the QC group and IDEOM confidence level of ≥ 5 were incorporated into a table and uploaded to MetaboAnalyst. Features with > 50% missing values were replaced by half of the minimum positive value in the original data. Interquantile range (IQR) were utilized to filter data, then $\log_2$ transformation and auto scaling were used to normalize the data. Principal component analysis (PCA) was performed to identify and remove outliers. PLSDA is normally used to reduce the dimension of variables from a large data set.(65) One-way ANOVA was used to identify metabolites with significant level changes between all samples and Fisher's least

square difference (LSD) to determine the metabolites with significant level changes between treatment and control groups. Statistically significant metabolites were selected using a false discovery rate of ≤ 0.1 for one-way ANOVA and $p \leq 0.05$ for Fisher's LSD. KEGG mapper was used to determine the pathway modules by statistically significant metabolites containing the KEGG compound numbers.

Acknowledgements

J.L. and T.V. are supported by research grants from the National Institute of Allergy and Infectious Diseases of the National Institutes of Health (R01 AI132681). J.L. and T.V. are also supported by the Australian National Health and Medical Research Council (NHMRC) as Principal Research and Career Development Level 2 Fellows, respectively. The content is solely the responsibility of the authors and does not necessarily represent the official views of the National Institute of Allergy and Infectious Diseases or the National Institutes of Health. The authors wish to thank the Monash Proteomics and Metabolomics Facility for sample analysis and particularly Amanda Peterson for technical assistance. The authors would like to thank Elena K. Schneider-Futschik for assistance with English grammar editing of the manuscript.

536

537

538

539

References

1. Organization WH. Global priority list of antibiotic-resistant bacteria to guide research, discovery, and development of new antibiotics. Geneva: WHO; 2017.
2. Boucher HW, Talbot GH, Bradley JS, Edwards JE, Gilbert D, Rice LB, Scheld M, Spellberg B, Bartlett J. 2009. Bad bugs, no drugs: no ESKAPE! An update from the Infectious Diseases Society of America. Clinical Infectious Diseases 48:1-12.
3. Rice LB. 2008. Federal funding for the study of antimicrobial resistance in nosocomial pathogens: no ESKAPE. The University of Chicago Press.
4. Lyczak JB, Cannon CL, Pier GB. 2002. Lung infections associated with cystic fibrosis. Clinical microbiology reviews 15:194-222.
5. Verkman A, Song Y, Thiagarajah JR. 2003. Role of airway surface liquid and submucosal glands in cystic fibrosis lung disease. American Journal of Physiology-Cell Physiology 284:C2-C15.
6. Moradali MF, Ghods S, Rehm BH. 2017. Pseudomonas aeruginosa lifestyle: a paradigm for adaptation, survival, and persistence. Frontiers in cellular and infection microbiology 7:39.
7. Lambert P. 2002. Mechanisms of antibiotic resistance in Pseudomonas aeruginosa. Journal of the royal society of medicine 95:22.
8. Lister PD, Wolter DJ, Hanson ND. 2009. Antibacterial-resistant Pseudomonas aeruginosa: clinical impact and complex regulation of chromosomally encoded resistance mechanisms. Clinical microbiology reviews 22:582-610.
9. Breidenstein EB, de la Fuente-Nunez C, Hancock RE. 2011. Pseudomonas aeruginosa: all roads lead to resistance. Trends Microbiol 19:419-26.
10. Li J, Nation RL, Turnidge JD, Milne RW, Coulthard K, Rayner CR, Paterson DL. 2006. Colistin: the re-emerging antibiotic for multidrug-resistant Gram-negative bacterial infections. Lancet Infect Dis 6:589-601.
11. Nation RL, Li J, Cars O, Couet W, Dudley MN, Kaye KS, Mouton JW, Paterson DL, Tam VH, Theuretzbacher U, Tsuji BT, Turnidge JD. 2015. Framework for optimisation of the clinical use of colistin and polymyxin B: the Prato polymyxin consensus. Lancet Infect Dis 15:225-34.
12. Velkov T, Roberts KD, Nation RL, Thompson PE, Li J. 2013. Pharmacology of polymyxins: new insights into an 'old'class of antibiotics. Future microbiology 8:711-724.
13. Hancock RE. 1984. Alterations in outer membrane permeability. Annual review of microbiology 38:237-264.
14. Hancock RE, Bell A. 1989. Antibiotic uptake into gram-negative bacteria, p 42-53, Perspectives in Antiinfective Therapy. Springer.
15. Trimble MJ, Mlynárčik P, Kolář M, Hancock RE. 2016. Polymyxin: alternative mechanisms of action and resistance. Cold Spring Harbor perspectives in medicine 6:a025288.
16. Li J, Rayner CR, Nation RL, Owen RJ, Spelman D, Tan KE, Liolios L. 2006. Heteroresistance to colistin in multidrug-resistant Acinetobacter baumannii. Antimicrobial agents and chemotherapy 50:2946-2950.
17. Bergen PJ, Bulman ZP, Saju S, Bulitta JB, Landersdorfer C, Forrest A, Li J, Nation RL, Tsuji BT. 2015. Polymyxin combinations: pharmacokinetics and pharmacodynamics for rationale use. Pharmacotherapy: The Journal of Human Pharmacology and Drug Therapy 35:34-42.
18. McPhee JB, Lewenza S, Hancock RE. 2003. Cationic antimicrobial peptides activate a two‐component regulatory system, PmrA‐PmrB, that regulates resistance to polymyxin B and cationic antimicrobial peptides in Pseudomonas aeruginosa. Molecular microbiology 50:205-217.
19. Gellatly SL, Needham B, Madera L, Trent MS, Hancock RE. 2012. The Pseudomonas aeruginosa PhoP-PhoQ two-component regulatory system is induced upon interaction with epithelial cells and controls cytotoxicity and inflammation. Infection and immunity 80:3122-3131.

20. Thaipisuttikul I, Hittle LE, Chandra R, Zangari D, Dixon CL, Garrett TA, Rasko DA, Dasgupta N, Moskowitz SM, Malmström L. 2014. A divergent P seudomonas aeruginosa palmitoyltransferase essential for cystic fibrosis‐specific lipid A. Molecular microbiology 91:158-174.
21. Lim TP, Lee W, Tan TY, Sasikala S, Teo J, Hsu LY, Tan TT, Syahidah N, Kwa AL. 2011. Effective antibiotics in combination against extreme drug-resistant Pseudomonas aeruginosa with decreased susceptibility to polymyxin B. PLoS One 6:e28177.
22. Kaddurah‐Daouk R, Weinshilboum RM. 2014. Pharmacometabolomics: implications for clinical pharmacology and systems pharmacology. Clinical Pharmacology & Therapeutics 95:154-167.
23. Mastrangelo A, G Armitage E, García A, Barbas C. 2014. Metabolomics as a tool for drug discovery and personalised medicine. A review. Current topics in medicinal chemistry 14:2627-2636.
24. Clish CB. 2015. Metabolomics: an emerging but powerful tool for precision medicine. Molecular Case Studies 1:a000588.
25. Emiola A, Andrews SS, Heller C, George J. 2016. Crosstalk between the lipopolysaccharide and phospholipid pathways during outer membrane biogenesis in Escherichia coli. Proceedings of the National Academy of Sciences 113:3108-3113.
26. Jeukens J, Freschi L, Kukavica-Ibrulj I, Emond-Rheault J-G, Tucker NP, Levesque RC. 2017. Genomics of antibiotic-resistance prediction in Pseudomonas aeruginosa. Annals of the New York Academy of Sciences.
27. Taber HW, Mueller J, Miller P, Arrow A. 1987. Bacterial uptake of aminoglycoside antibiotics. Microbiological reviews 51:439.
28. Bergen PJ, Bulitta JB, Forrest A, Tsuji BT, Li J, Nation RL. 2010. Pharmacokinetic/pharmacodynamic investigation of colistin against Pseudomonas aeruginosa using an in vitro model. Antimicrobial agents and chemotherapy 54:3783-3789.
29. Matthaiou DK, Michalopoulos A, Rafailidis PI, Karageorgopoulos DE, Papaioannou V, Ntani G, Samonis G, Falagas ME. 2008. Risk factors associated with the isolation of colistin-resistant gram-negative bacteria: a matched case-control study. Critical care medicine 36:807-811.
30. Hancock RE, Chapple DS. 1999. Peptide antibiotics. Antimicrobial agents and chemotherapy 43:1317-1323.
31. Han M-L, Zhu Y, Creek DJ, Lin Y-W, Anderson D, Shen H-H, Tsuji B, Gutu AD, Moskowitz SM, Velkov T. 2018. Alterations of metabolic and lipid profiles in polymyxin-resistant Pseudomonas aeruginosa. Antimicrobial agents and chemotherapy 62:e02656-17.
32. Hussein M, Han M-L, Zhu Y, Schneider-Futschik EK, Hu X, Zhou QT, Lin Y-W, Anderson D, Creek DJ, Hoyer D. 2018. Mechanistic Insights From Global Metabolomics Studies into Synergistic Bactericidal Effect of a Polymyxin B Combination With Tamoxifen Against Cystic Fibrosis MDR Pseudomonas aeruginosa. Computational and structural biotechnology journal 16:587-599.
33. Henry R, Crane B, Powell D, Deveson Lucas D, Li Z, Aranda J, Harrison P, Nation RL, Adler B, Harper M. 2015. The transcriptomic response of Acinetobacter baumannii to colistin and doripenem alone and in combination in an in vitro pharmacokinetics/pharmacodynamics model. Journal of Antimicrobial Chemotherapy 70:1303-1313.
34. Louesdon S, Charlot‐Rougé S, Tourdot‐Maréchal R, Bouix M, Béal C. 2015. Membrane fatty acid composition and fluidity are involved in the resistance to freezing of Lactobacillus buchneri R1102 and Bifidobacterium longum R0175. Microbial biotechnology 8:311-318.
35. Nikaido H, Hancock R. 1986. Outer membrane permeability of Pseudomonas aeruginosa. The bacteria 10:145-193.
36. Mansilla MC, Cybulski LE, Albanesi D, de Mendoza D. 2004. Control of membrane lipid fluidity by molecular thermosensors. Journal of bacteriology 186:6681-6688.

37. Kotra LP, Haddad J, Mobashery S. 2000. Aminoglycosides: perspectives on mechanisms of action and resistance and strategies to counter resistance. Antimicrobial agents and chemotherapy 44:3249-3256.
38. Bera S, Zhanel GG, Schweizer F. 2010. Antibacterial activities of aminoglycoside antibiotics-derived cationic amphiphiles. Polyol-modified neomycin B-, kanamycin A-, amikacin-, and neamine-based amphiphiles with potent broad spectrum antibacterial activity. Journal of medicinal chemistry 53:3626-3631.
39. Sautrey G, El Khoury M, dos Santos AG, Zimmermann L, Deleu M, Lins L, Décout J-L, Mingeot-Leclercq M-P. 2016. Negatively Charged Lipids as a Potential Target for New Amphiphilic Aminoglycoside Antibiotics A BIOPHYSICAL STUDY. Journal of Biological Chemistry 291:13864-13874.
40. Zhang Y-M, Rock CO. 2008. Membrane lipid homeostasis in bacteria. Nature Reviews Microbiology 6:222.
41. Velkov T, Roberts KD, Nation RL, Wang J, Thompson PE, Li J. 2014. Teaching 'old'polymyxins new tricks: new-generation lipopeptides targeting Gram-negative 'superbugs'. ACS chemical biology 9:1172-1177.
42. Brade H. 1999. Endotoxin in health and disease. CRC Press.
43. Gourlay LJ, Sommaruga S, Nardini M, Sperandeo P, Deho G, Polissi A, Bolognesi M. 2010. Probing the active site of the sugar isomerase domain from E. coli arabinose‐5‐phosphate isomerase via X‐ray crystallography. Protein Science 19:2430-2439.
44. Taylor PL, Blakely KM, De Leon GP, Walker JR, McArthur F, Evdokimova E, Zhang K, Valvano MA, Wright GD, Junop MS. 2008. Structure and function of sedoheptulose-7-phosphate isomerase, a critical enzyme for lipopolysaccharide biosynthesis and a target for antibiotic adjuvants. Journal of Biological Chemistry 283:2835-2845.
45. Brooke JS, Valvano M. 1996. Molecular cloning of the Haemophilus influenzae gmhA (lpcA) gene encoding a phosphoheptose isomerase required for lipooligosaccharide biosynthesis. Journal of bacteriology 178:3339-3341.
46. Murima P, McKinney JD, Pethe K. 2014. Targeting bacterial central metabolism for drug development. Chemistry & biology 21:1423-1432.
47. Wolfe AJ. 2015. Glycolysis for the microbiome generation. Microbiology spectrum 3.
48. Gest H. Evolutionary roots of the citric acid cycle in prokaryotes, p 3-16. *In* (ed),
49. Owen OE, Kalhan SC, Hanson RW. 2002. The key role of anaplerosis and cataplerosis for citric acid cycle function. Journal of Biological Chemistry 277:30409-30412.
50. Galeazzi L, Bocci P, Amici A, Brunetti L, Ruggieri S, Romine M, Reed S, Osterman AL, Rodionov DA, Sorci L. 2011. Identification of nicotinamide mononucleotide deamidase of the bacterial pyridine nucleotide cycle reveals a novel broadly conserved amidohydrolase family. Journal of Biological Chemistry 286:40365-40375.
51. Neidhardt FC, Ingraham JL, Schaechter M. 1990. Physiology of the bacterial cell: a molecular approach, vol 20. Sinauer Associates Sunderland, MA.
52. Dörries K, Schlueter R, Lalk M. 2014. Impact of antibiotics with various target sites on the metabolome of Staphylococcus aureus. Antimicrobial agents and chemotherapy 58:7151-7163.
53. Belenky P, Jonathan DY, Porter CB, Cohen NR, Lobritz MA, Ferrante T, Jain S, Korry BJ, Schwarz EG, Walker GC. 2015. Bactericidal antibiotics induce toxic metabolic perturbations that lead to cellular damage. Cell reports 13:968-980.
54. Perkins HR, Nieto M. 1973. The significance of D-alanyl-D-alanine termini in the biosynthesis of bacterial cell walls and the action of penicillin, vancomycin and ristocetin. Pure and Applied Chemistry 35:371-382.
55. Milewski S. 2002. Glucosamine-6-phosphate synthase—the multi-facets enzyme. Biochimica et Biophysica Acta (BBA)-Protein Structure and Molecular Enzymology 1597:173-192.

56. Maifiah MHM, Creek DJ, Nation RL, Forrest A, Tsuji BT, Velkov T, Li J. 2017. Untargeted metabolomics analysis reveals key pathways responsible for the synergistic killing of colistin and doripenem combination against Acinetobacter baumannii. Scientific Reports 7:45527.
57. Han M-L, Zhu Y, Creek DJ, Lin Y-W, Gutu AD, Hertzog P, Purcell T, Shen H-H, Moskowitz SM, Velkov T. 2019. Comparative Metabolomics and Transcriptomics Reveal Multiple Pathways Associated with Polymyxin Killing in Pseudomonas aeruginosa. MSystems 4:e00149-18.
58. Xiong L, Teng JL, Botelho MG, Lo RC, Lau SK, Woo PC. 2016. Arginine metabolism in bacterial pathogenesis and cancer therapy. International journal of molecular sciences 17:363.
59. Anonymous. 2016. Cold Spring Protocols doi:10.1101/pdb.rec088559. CSH Laboratories, Woodbury NY.
60. Gika HG, Theodoridis GA, Wingate JE, Wilson ID. 2007. Within-day reproducibility of an HPLC-MS-based method for metabonomic analysis: application to human urine. J Proteome Res 6:3291-303.
61. Zhang T, Creek DJ, Barrett MP, Blackburn G, Watson DG. 2012. Evaluation of coupling reversed phase, aqueous normal phase, and hydrophilic interaction liquid chromatography with Orbitrap mass spectrometry for metabolomic studies of human urine. Anal Chem 84:1994-2001.
62. Creek DJ, Jankevics A, Burgess KE, Breitling R, Barrett MP. 2012. IDEOM: an Excel interface for analysis of LC-MS-based metabolomics data. Bioinformatics 28:1048-9.
63. Scheltema RA, Jankevics A, Jansen RC, Swertz MA, Breitling R. 2011. PeakML/mzMatch: a file format, Java library, R library, and tool-chain for mass spectrometry data analysis. Anal Chem 83:2786-93.
64. Smith CA, Want EJ, O'Maille G, Abagyan R, Siuzdak G. 2006. XCMS: Processing mass spectrometry data for metabolite profiling using Nonlinear peak alignment, matching, and identification. Anal Chem 78:779-787.
65. Boulesteix A-L, Strimmer K. 2006. Partial least squares: a versatile tool for the analysis of high-dimensional genomic data. Briefings in bioinformatics 8:32-44.

Figure captions

Figure 1. Perturbations of bacterial lipids. **(A)** Significantly perturbed lipids in *P. aeruginosa* FADDI-PA111 following treatment with polymyxin B (PMB, red), amikacin (AMK, green) and the combination (COM, purple) at **(i)** 15 min, **(ii)** 1 h, and **(iii)** 4 h. Lipid names are putatively assigned based on accurate mass. **(B)** Bar charts show the depletion of essential bacterial membrane lipids after treatment with polymyxin B, amikacin, and the combination across all three time points. ($\geq$ 1.0-$\log_2$-fold, $p \leq 0.05$; FDR ≤ 0.1).

Figure 2. Impact of the treatment on lipopolysaccharides biosynthesis. **(A)** Bar charts for significantly perturbed intermediates of PPP and downstream LPS in *P. aeruginosa* FADDI-PA111 following treatment with polymyxin B (PMB, red), amikacin (AMK, green) and the

combination (COM, purple) at 15 min. **(B) (i)** Schematic diagram and bar charts, and **(ii)** volcano plots for the significantly impacted intermediates of LPS biogenesis in *P. aeruginosa* FADDI-PA111 after treatment with polymyxin B, amikacin, and the combination at 1 h and **(C)** at 4h. ($\geq$ 1.0-$\log_2$-fold, $p \leq 0.05$; FDR ≤ 0.05).

Figure 3. The changes in central carbon metabolism. **(A)** Schematic diagram for the significantly perturbed intermediates of PPP, glycolysis and interrelated tricarboxylic cycle in *P. aeruginosa* FADDI-PA111 following treatment with polymyxin B (PMB, red), amikacin (AMK, green) and the combination (COM, purple) at 1 h. **(B)** Bar graphs for the main intermediates of PPP, glycolysis and TCA after treatment with polymyxin B, amikacin, and the combination at 1 h. ($\geqslant$ 1.0-$\log_2$-fold, $p \leqslant 0.05$; FDR $\leqslant 0.05$).

Figure 4. Perturbations of pyridine nucleotide cycle (PNC). **(A)** Schematic diagram for the significantly perturbed intermediates of PNC in *P. aeruginosa* FADDI-PA111 following treatment with polymyxin B (PMB, red), amikacin (AMK, green) and the combination (COM, purple) at 15 min. **(B)** Bar graphs for the main depleted precursors of PNC after treatment with polymyxin B, amikacin, and the combination at **(i)** 15 min and **(ii)** 1 h ($\geqslant$ 1.0-$\log_2$-fold, $p \leqslant 0.05$; FDR $\leqslant 0.1$).

Figure 5. Induction of nucleotides turnover and DNA damage. **(A)** Volcano plots for the significantly perturbed nucleotides at 15 min **(i)** and 1 h **(ii)** in *P. aeruginosa* FADDI-PA111 following treatment with polymyxin B (PMB, red), amikacin (AMK, green) and the combination (COM, purple). **(B)** Bars graphs for the nucleotides after treatment with polymyxin B, amikacin, and the combination at 4 h ($\geq$ 1.0-$\log_2$-fold, $p \leq 0.05$; FDR ≤ 0.1).

Figure 6. Changes in amino acids metabolism in FADDI-PA111. **(A)** Fold changes for the significantly affected amino acids **(i)** and bar charts of peptidoglycan intermediates **(ii)** following treatment with polymyxin B (PMB, red), amikacin (AMK, green) and the

752 combination (COM, purple) at 15 min. **(B)** Fold changes of significantly perturbed amino
753 acids **(i)** and bar graphs for intermediates of **(ii)** peptidoglycan biosynthesis and **(iii)** arginine
754 metabolism after treatment with polymyxin B, amikacin, and the combination at 1 h (≥ 1.0-
755 log_2-fold, $p \leq 0.05$; FDR ≤ 0.1). **(C)** Fold changes of significant amino acids metabolites at 4
756 h (≥ 1.0-log_2-fold, $p \leq 0.05$; FDR ≤ 0.1).

757 **Figure 7.** The significantly affected metabolites of peptides metabolism in FADDI-PA111.
758 Fold changes for the significantly affected peptides following treatment with polymyxin B
759 (PMB, red), amikacin (AMK, green) and the combination (COM, purple) at **(A)**15 min, **(B)** 1
760 h and **(C)** 4 h (≥ 1.0-log_2-fold, $p \leq 0.05$; FDR ≤ 0.1).

761

762

763

Figure 1

A.765

i. 766

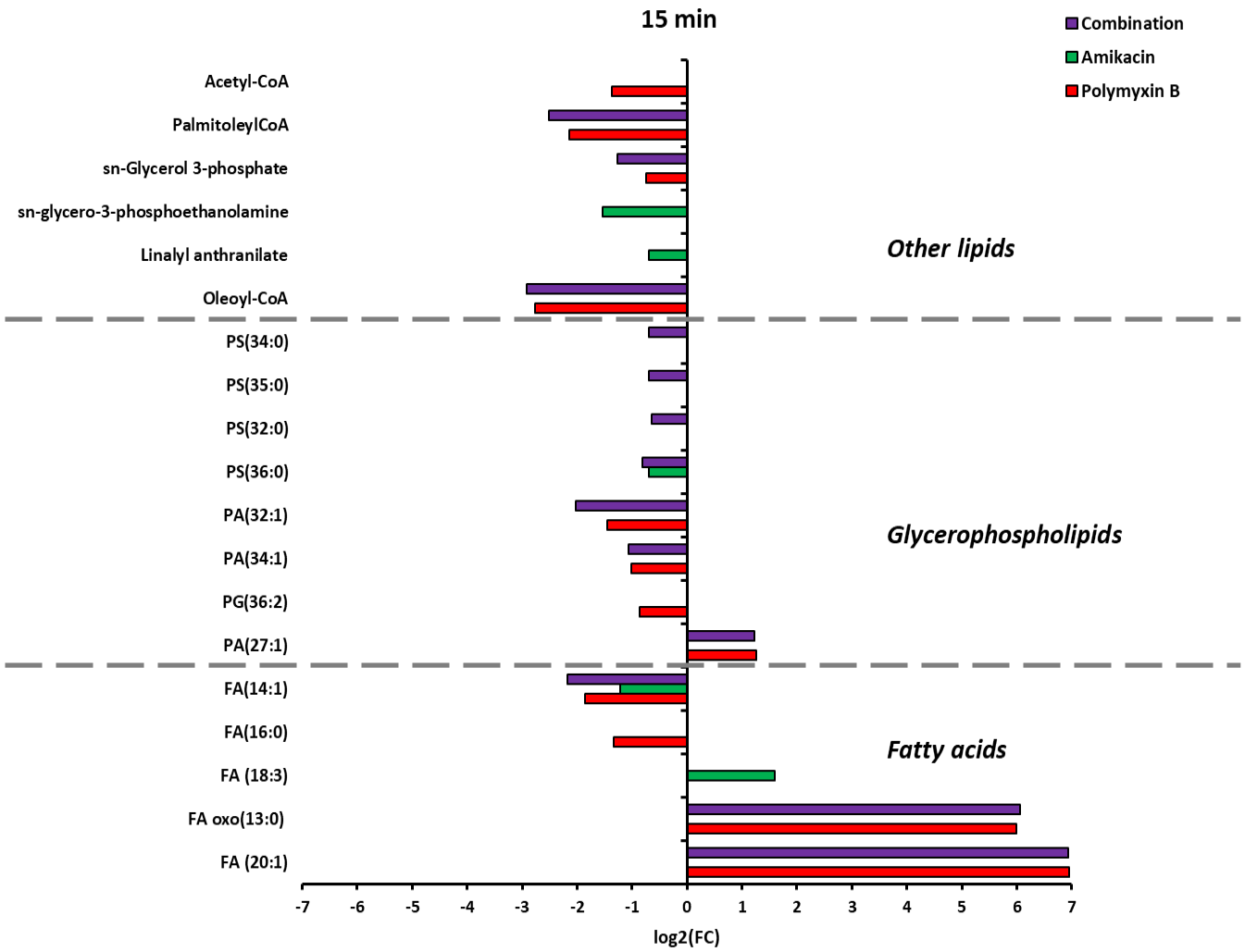

767

768

769

ii. 770

Antimicrobial Agents and Chemotherapy

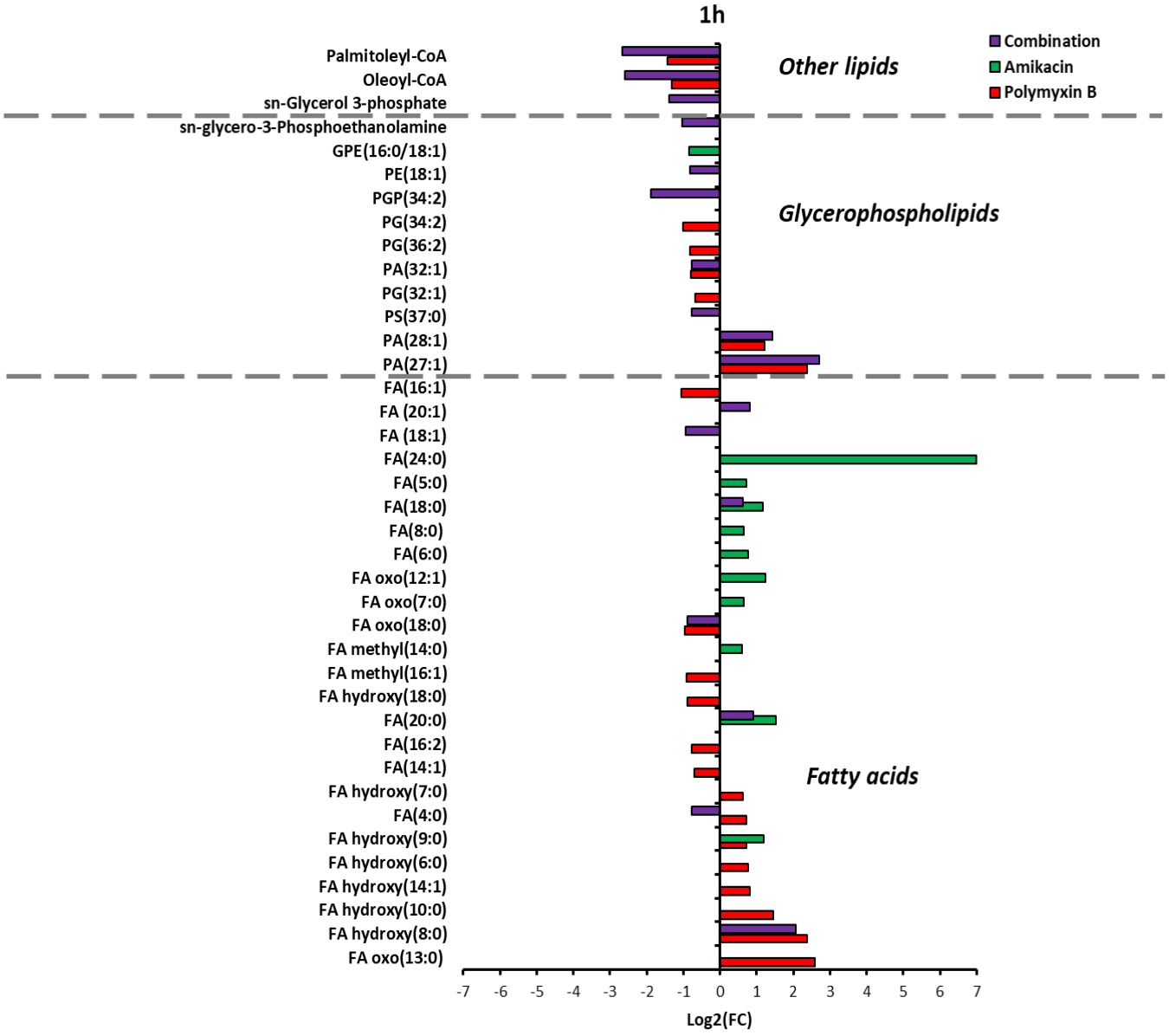

771

772

773

774

iii.

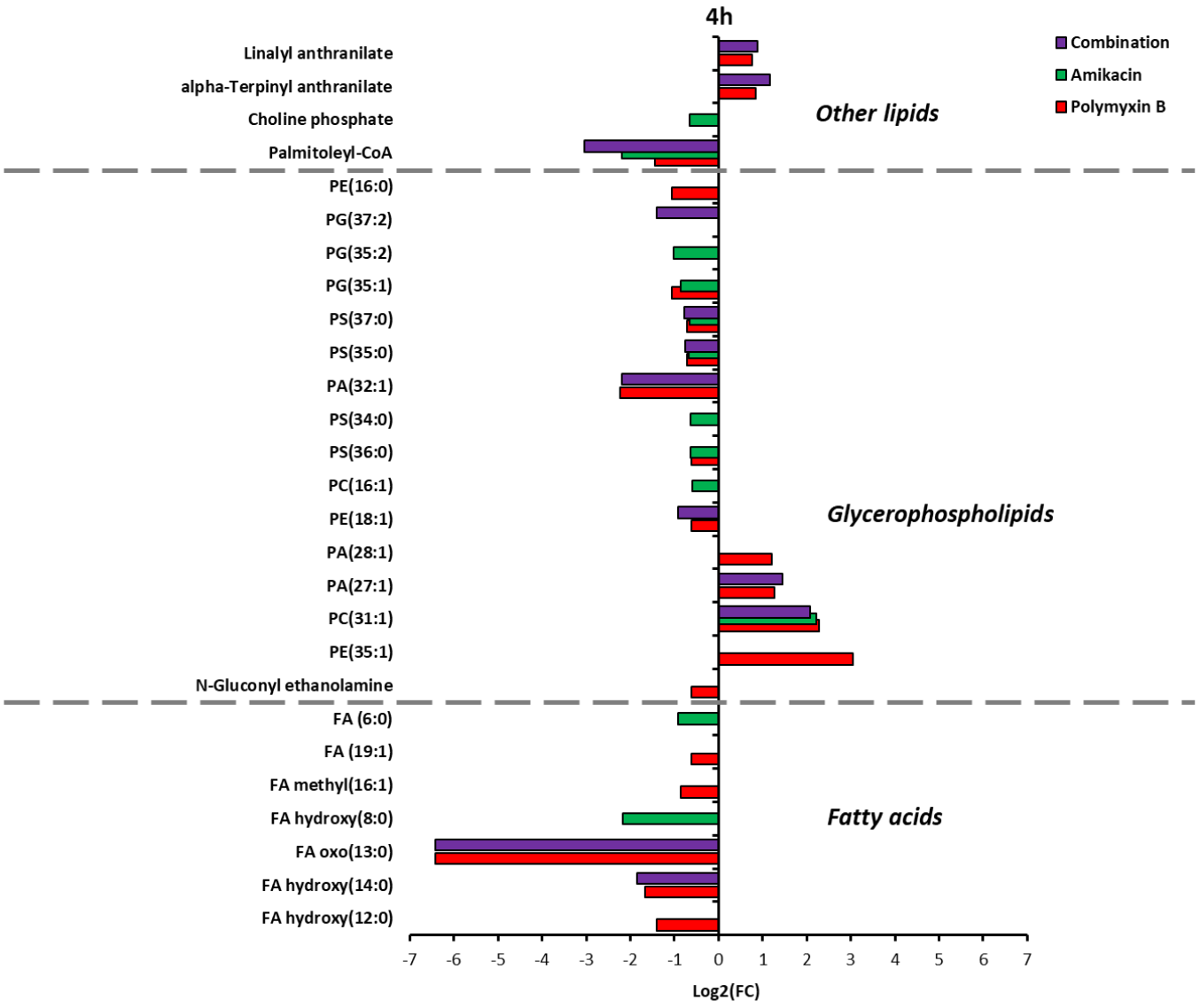

B.

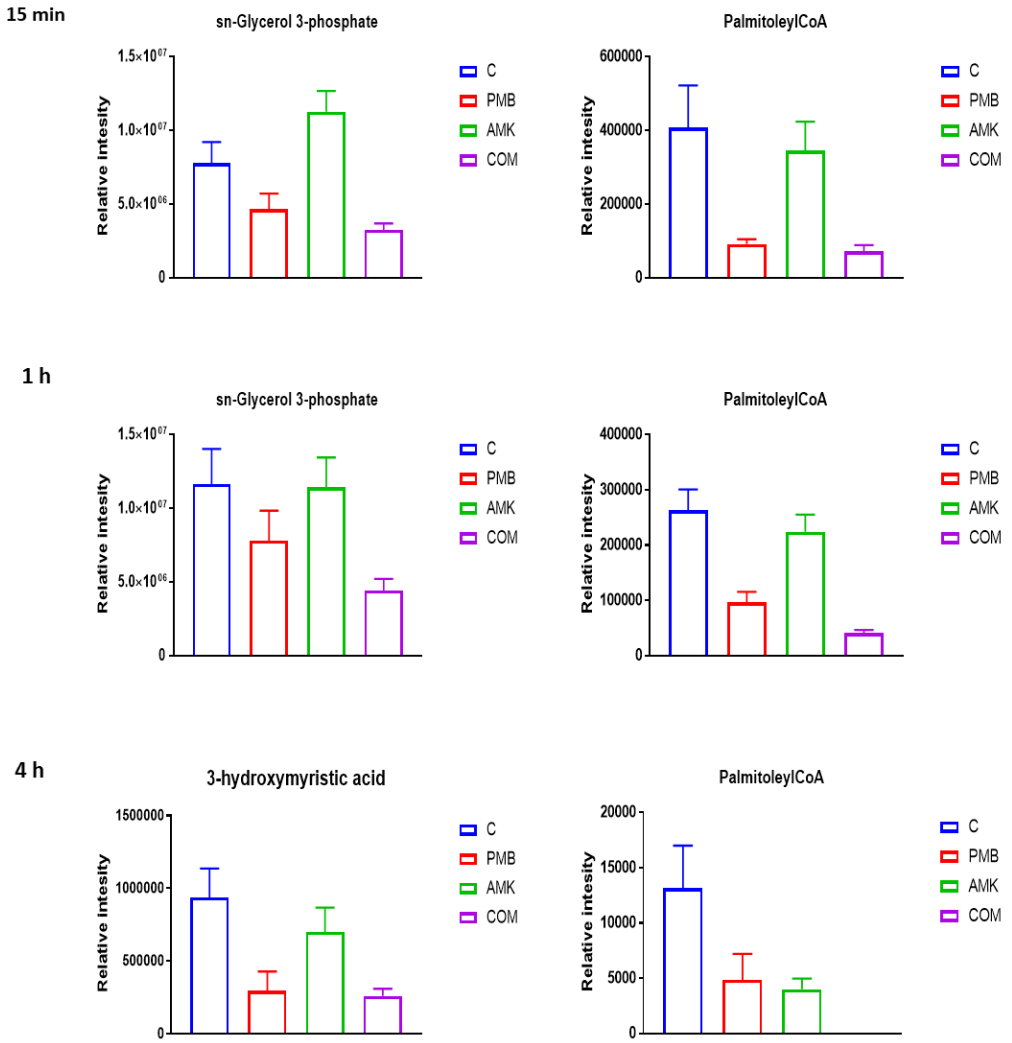

Figure 2

A.

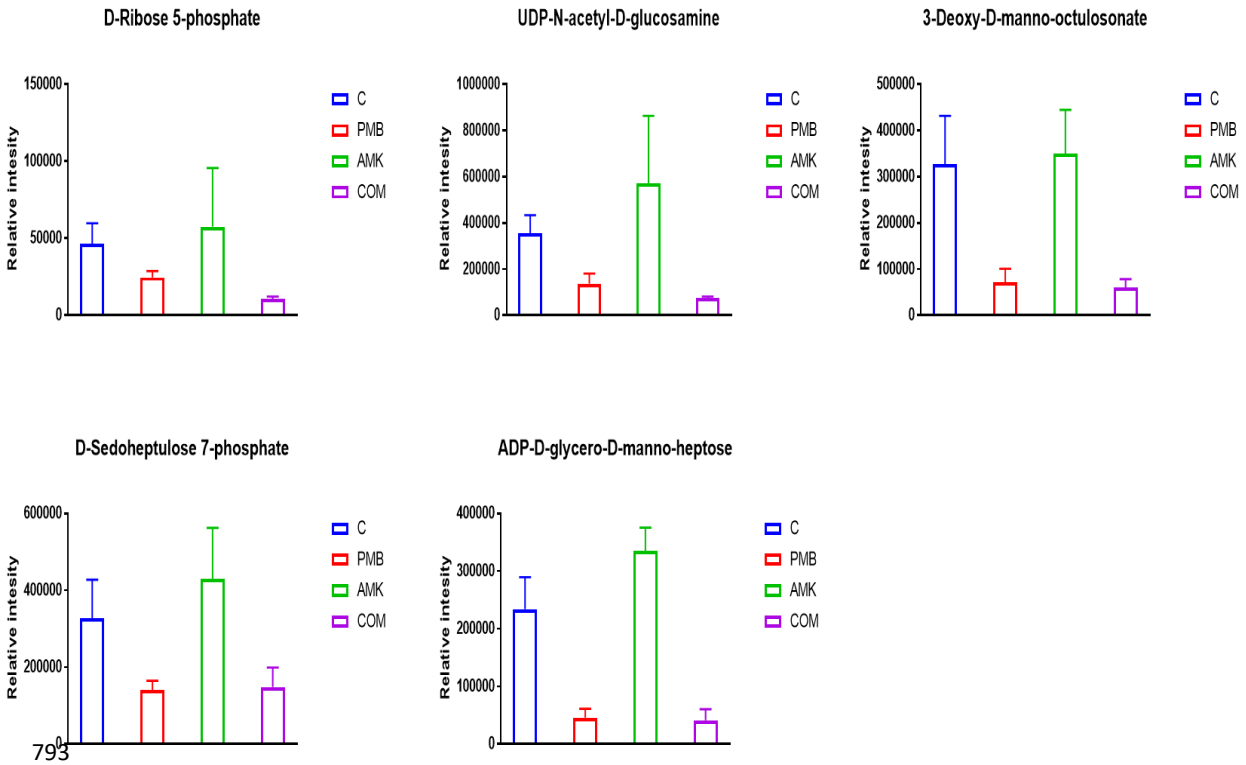

B. 801

i. 802

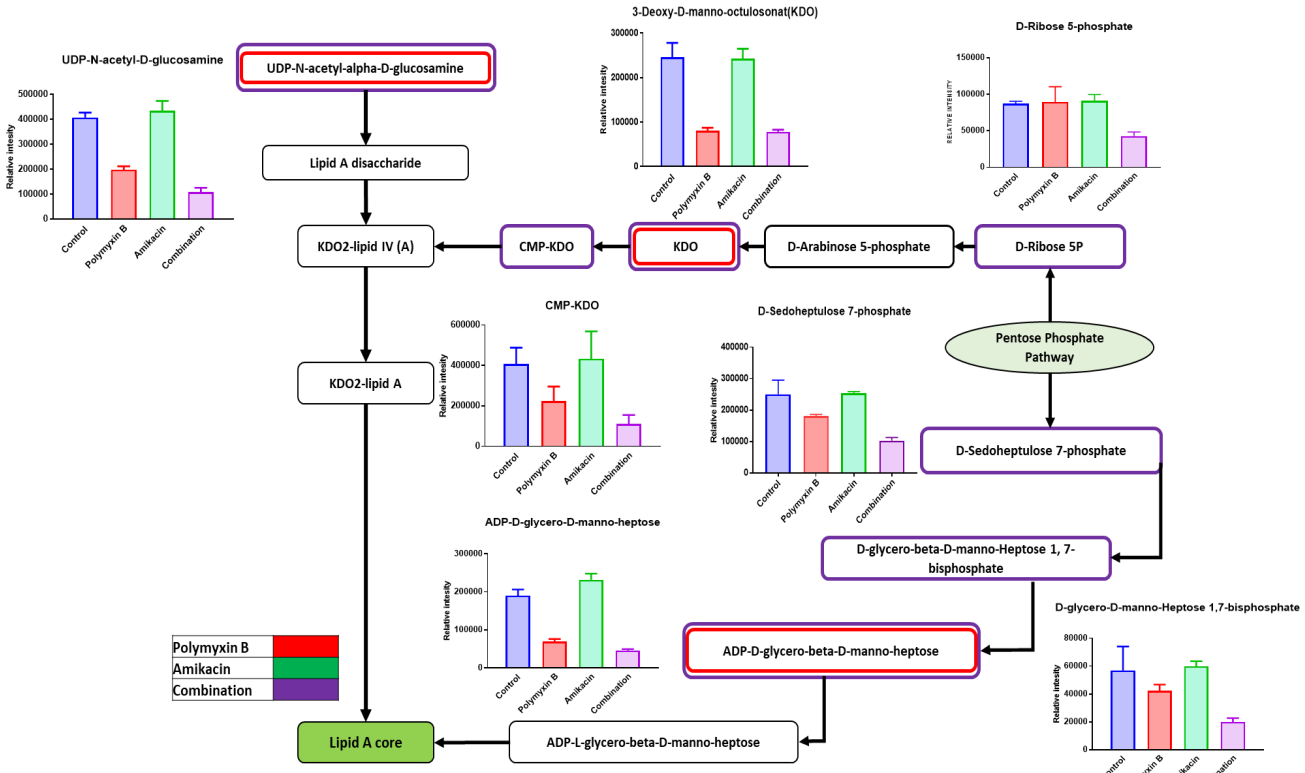

803

804

805

806

807

808

809

810

Antimicrobial Agents and Chemotherapy

B. 811

ii. 812

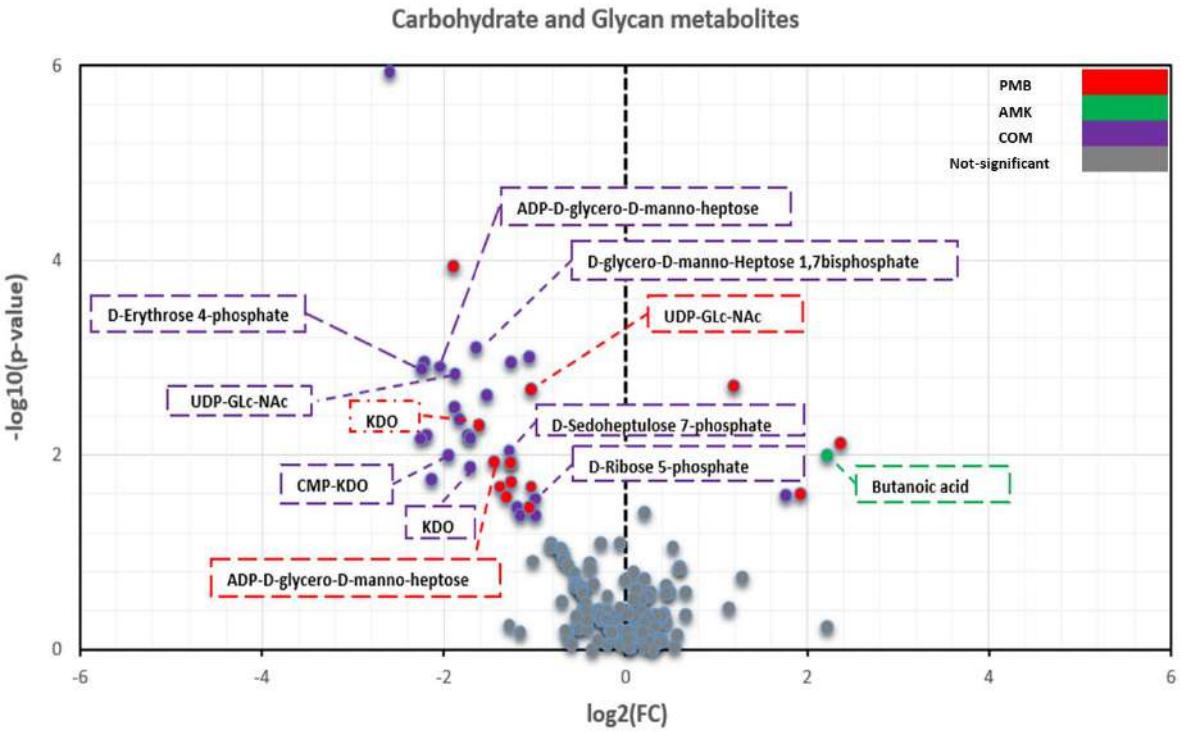

814

815

816

817

818

819

820

C.821

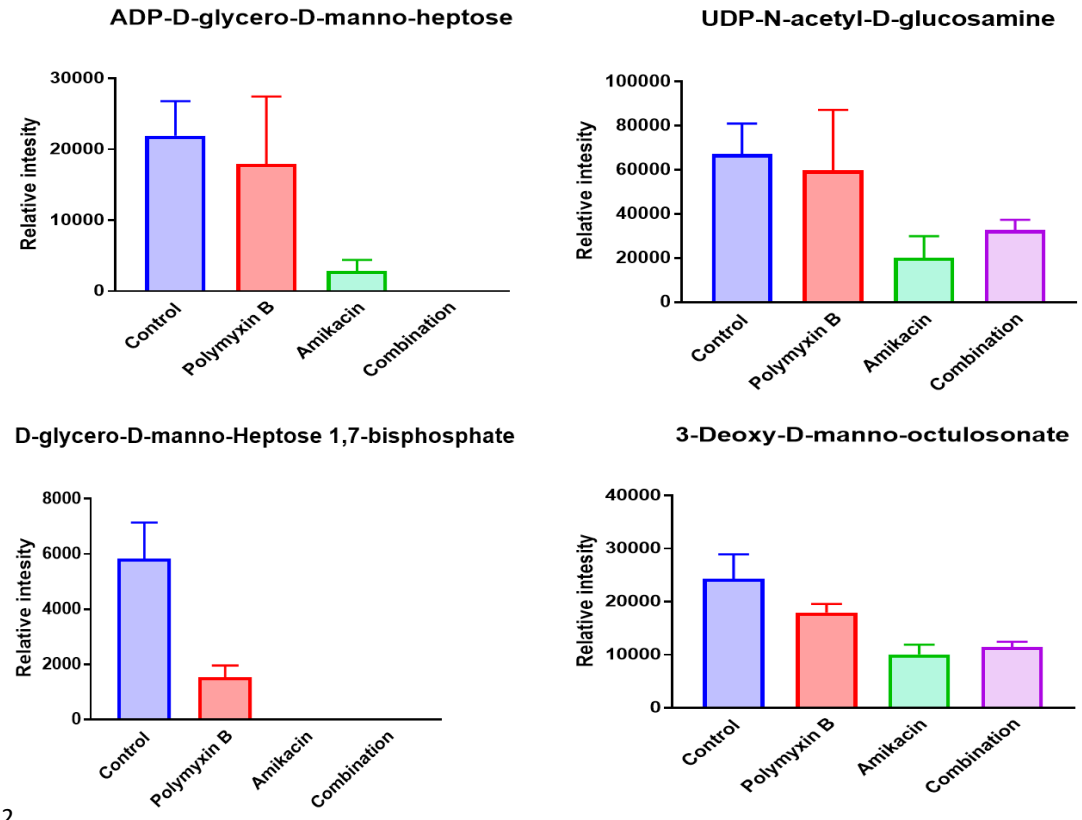

822

823

824

825

826

827

828

829

830

Figure 3 A.

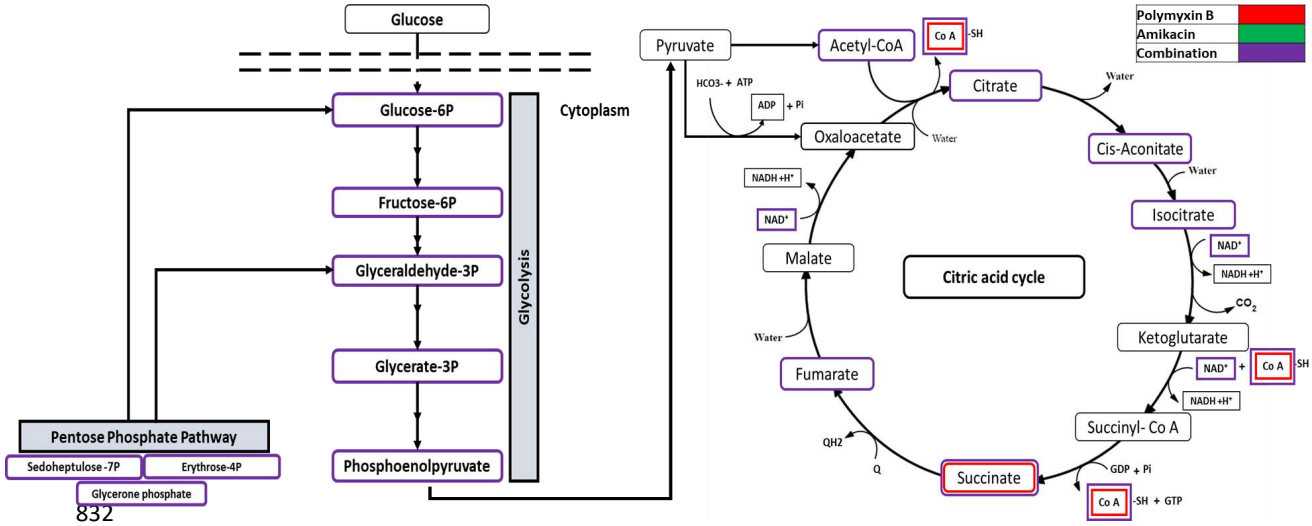

832

B. 833

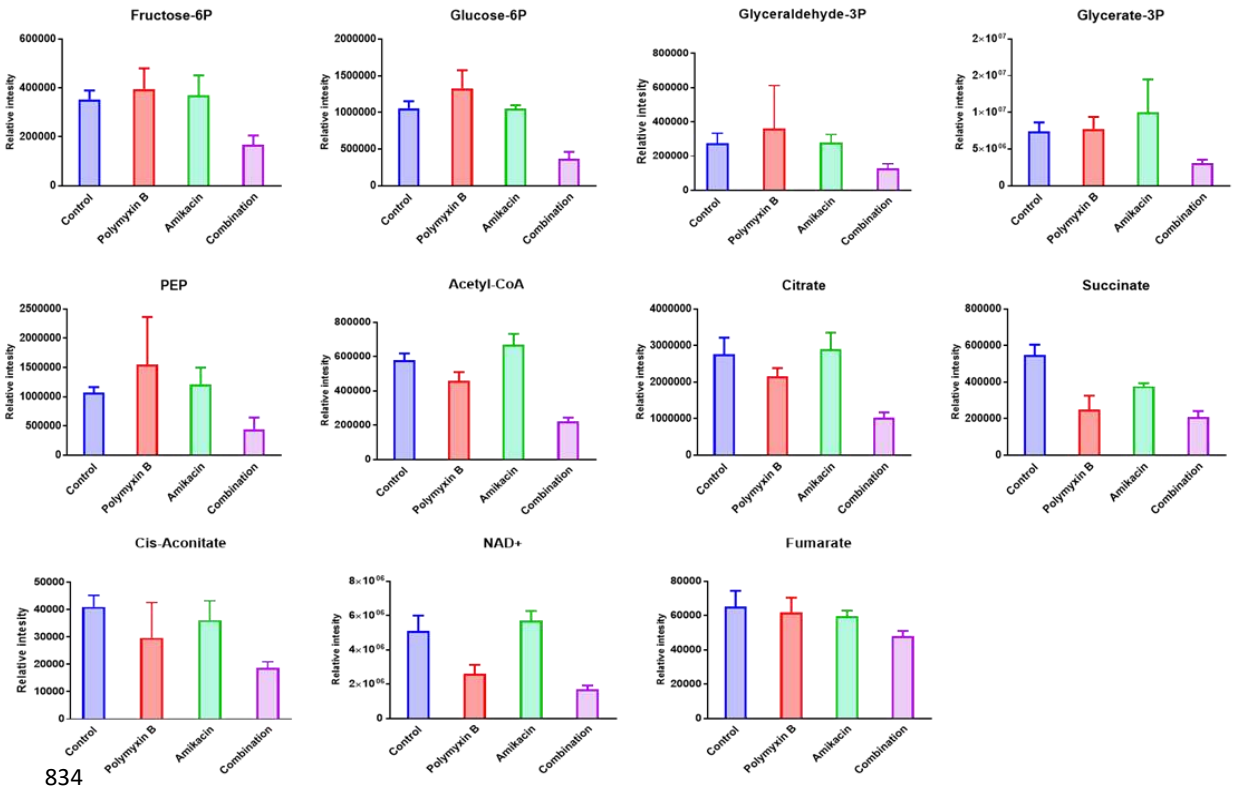

834

Figure 4

A.

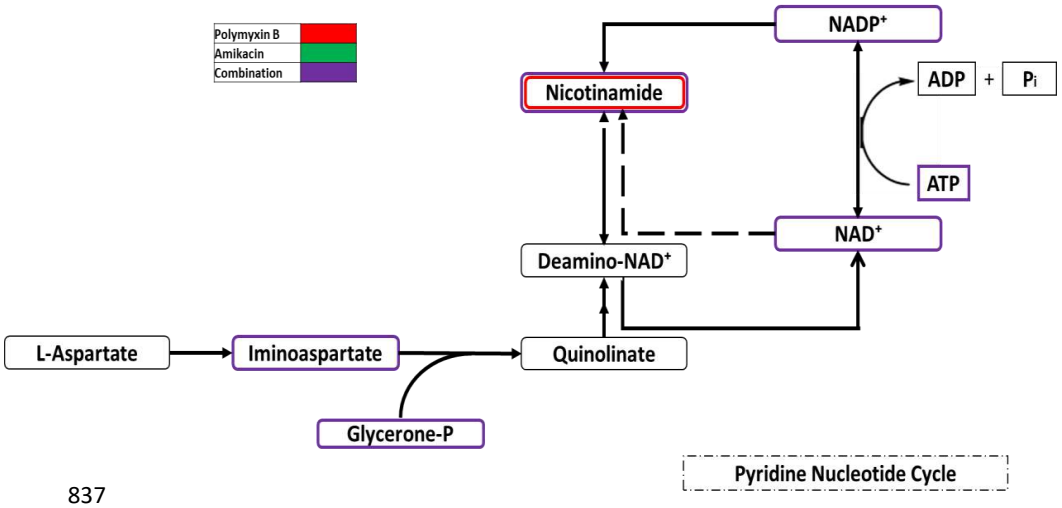

B.

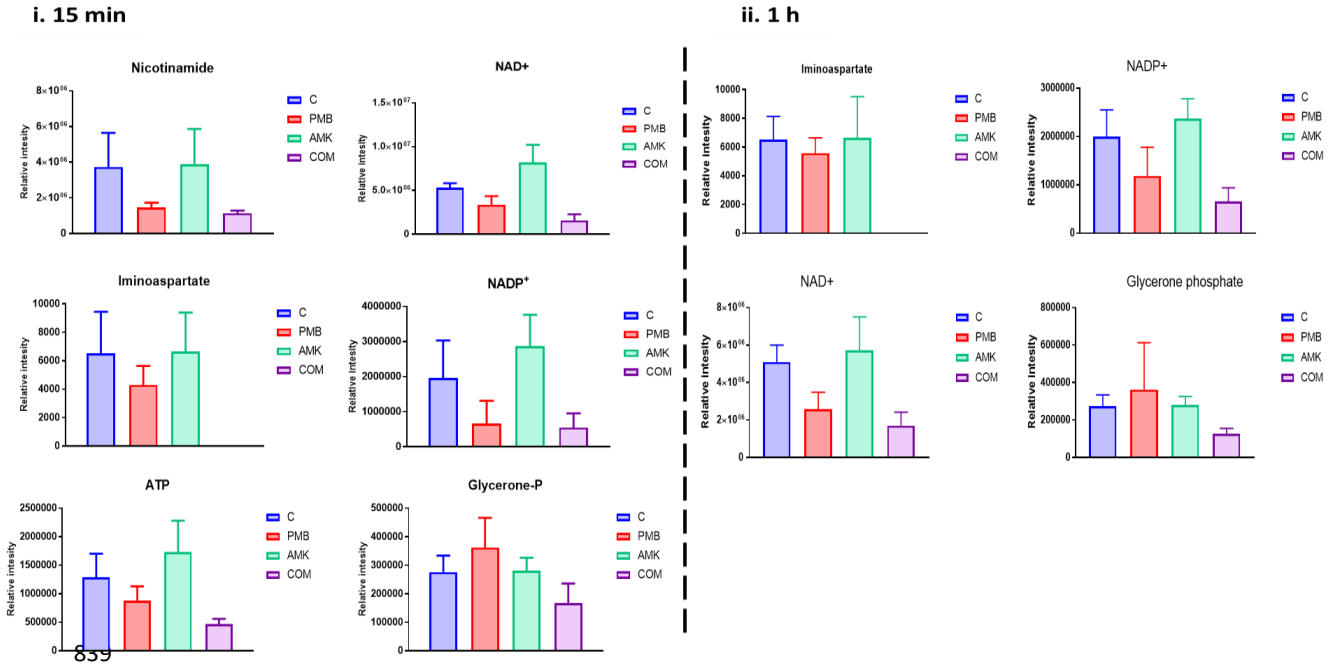

Figure 5

A.

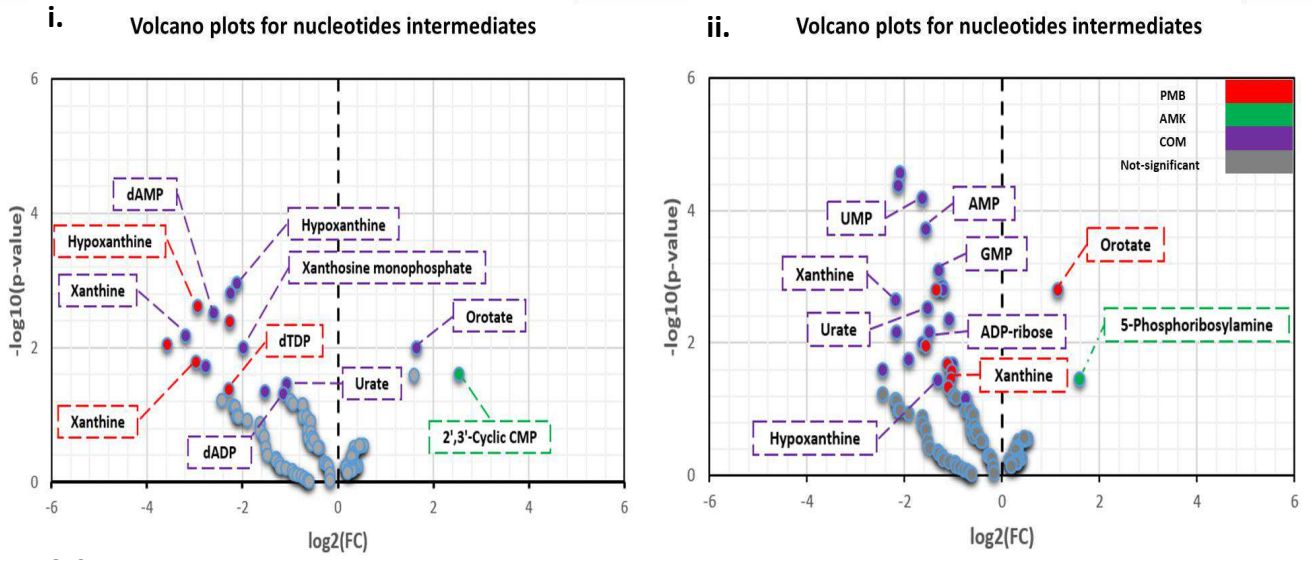

B.

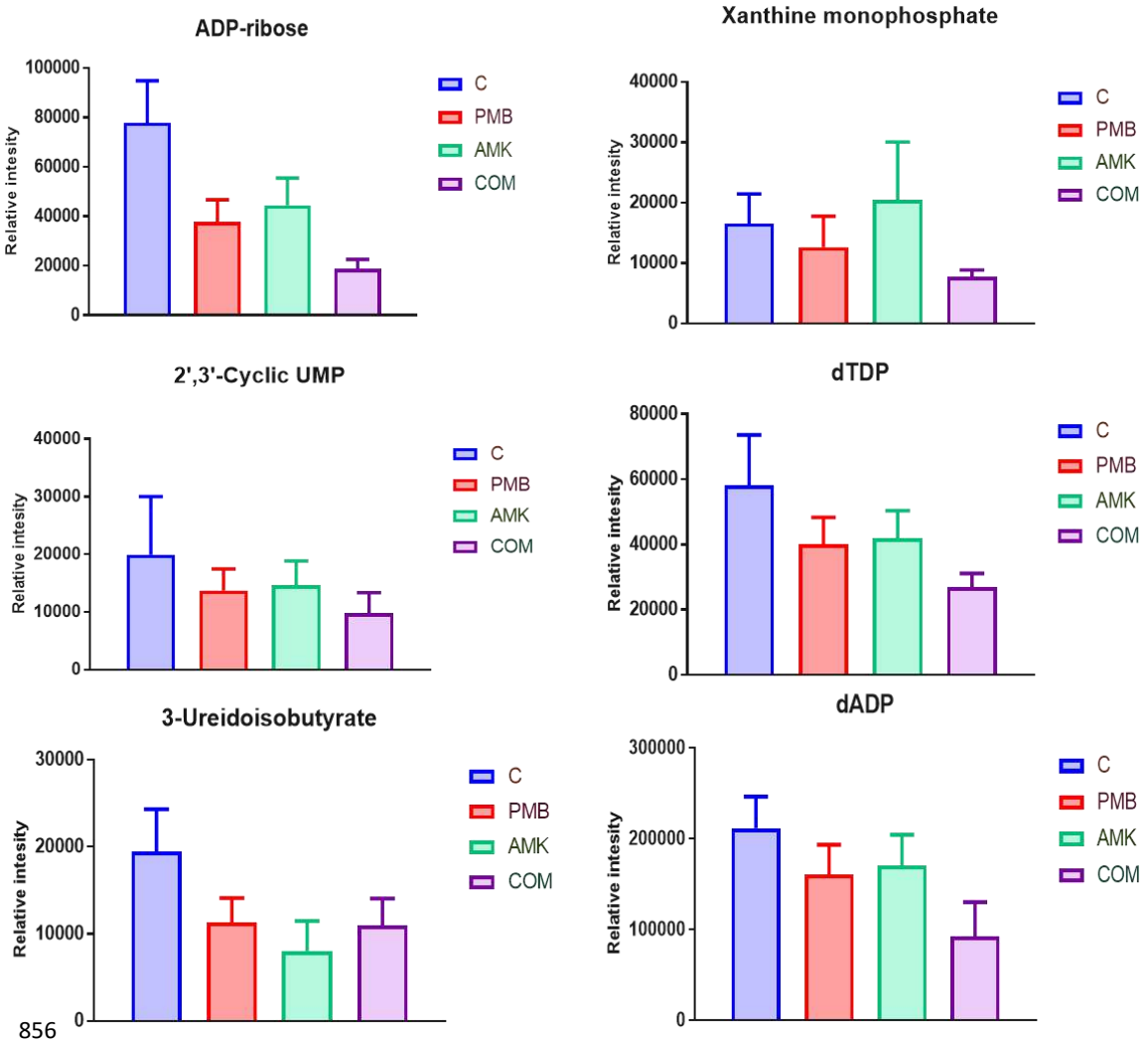

Figure 6

A. i.

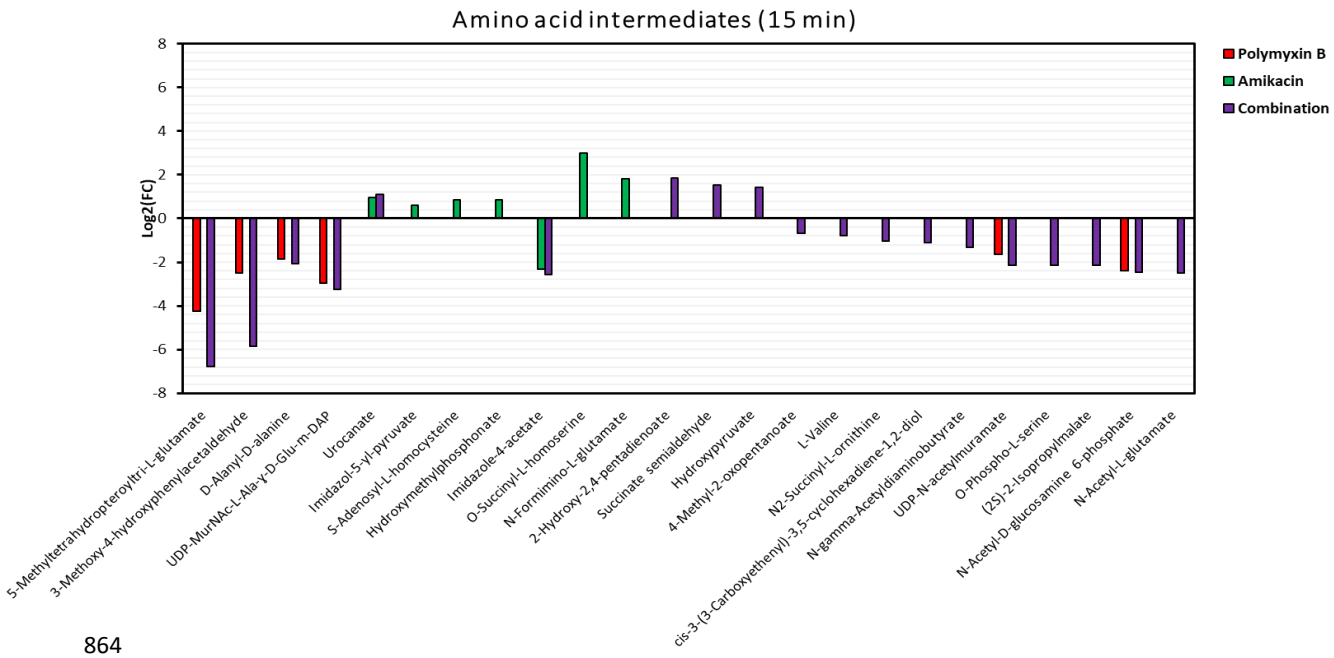

ii.

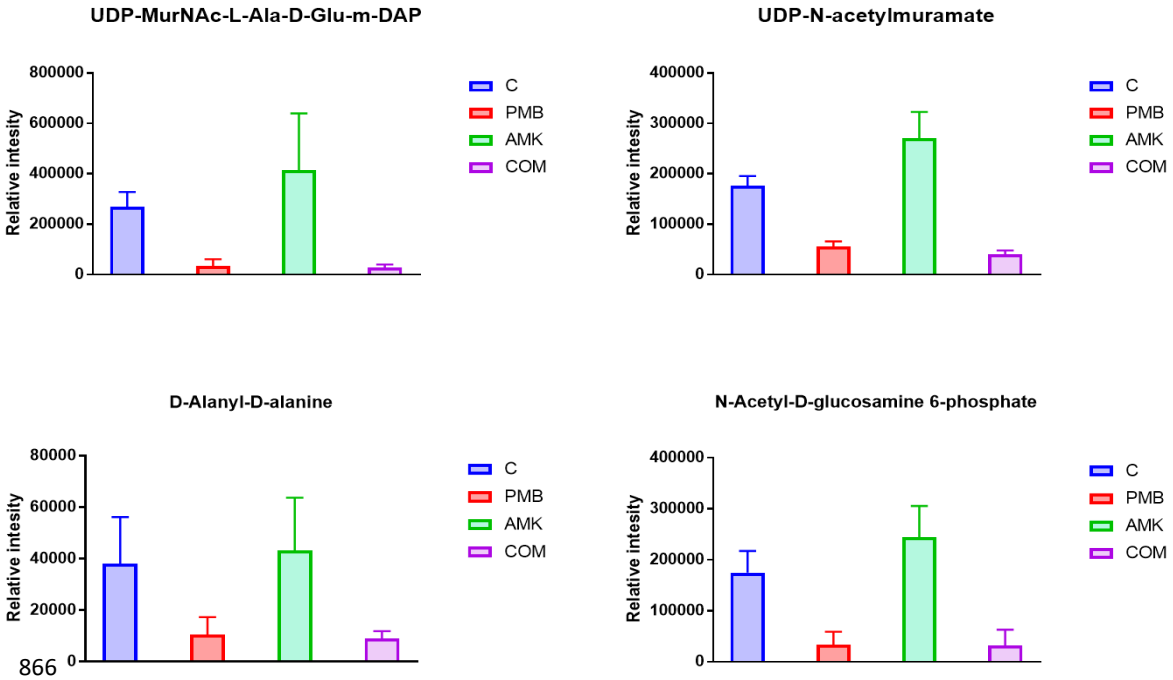

B. 867

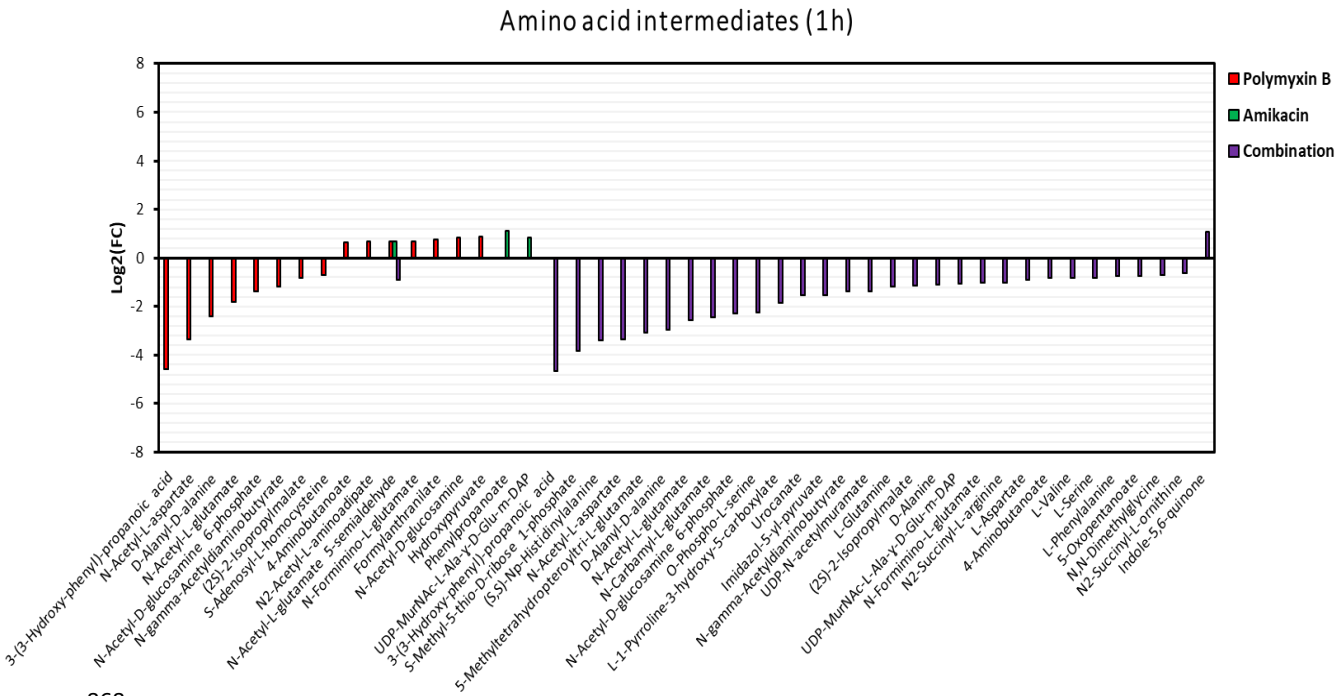

868

ii. 869

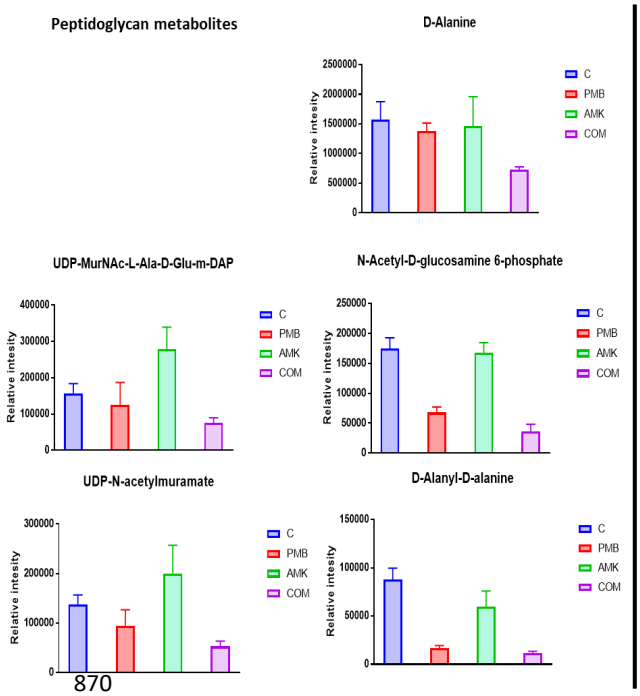

870

iii.

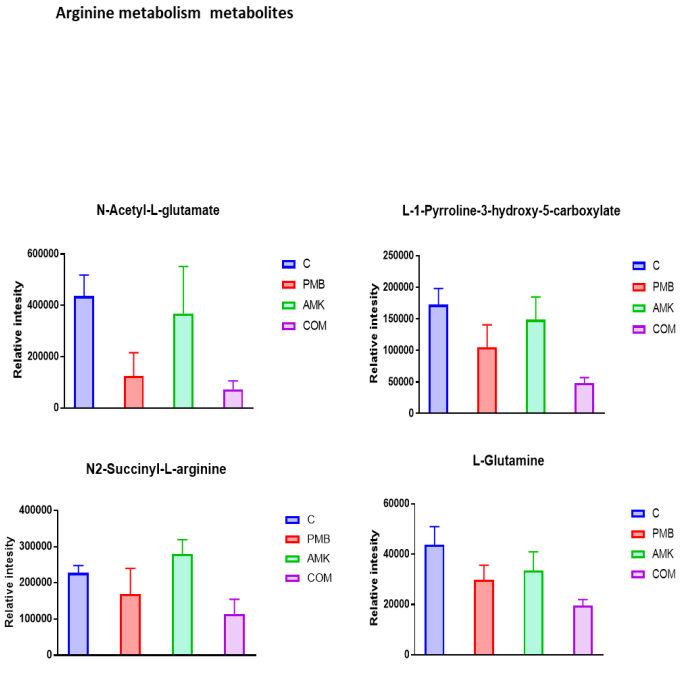

C.871

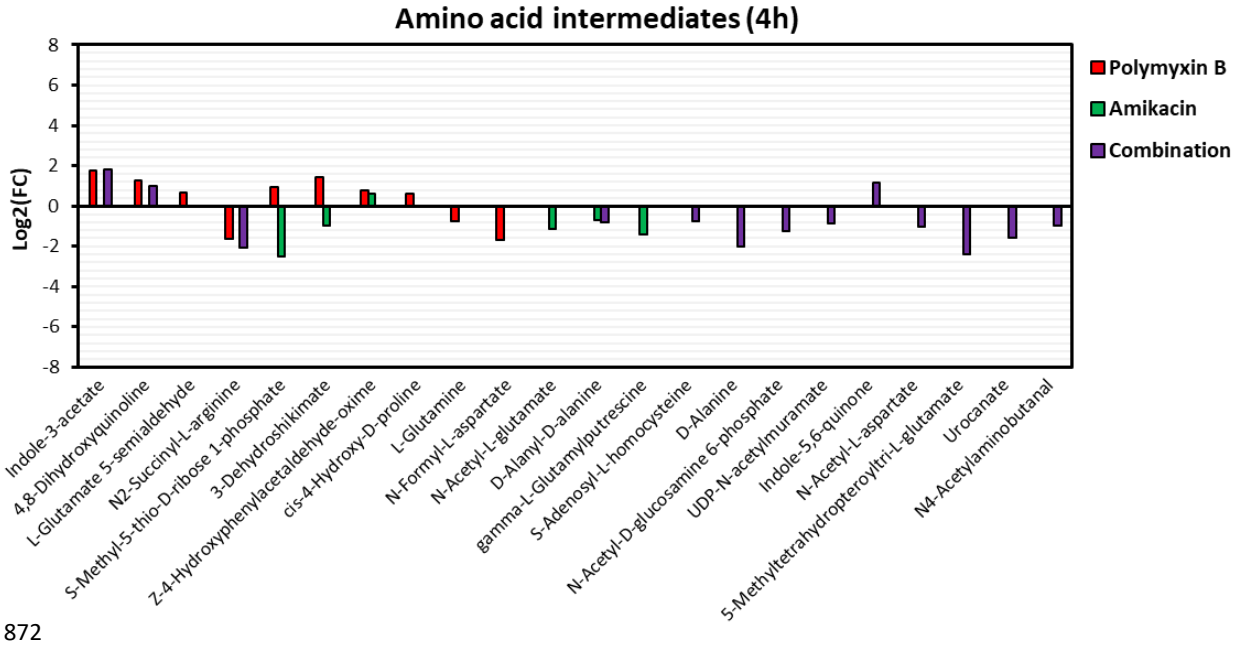

872

873

874

875

876

877

878

879

880

881

882

883

884

Figure 7

A.

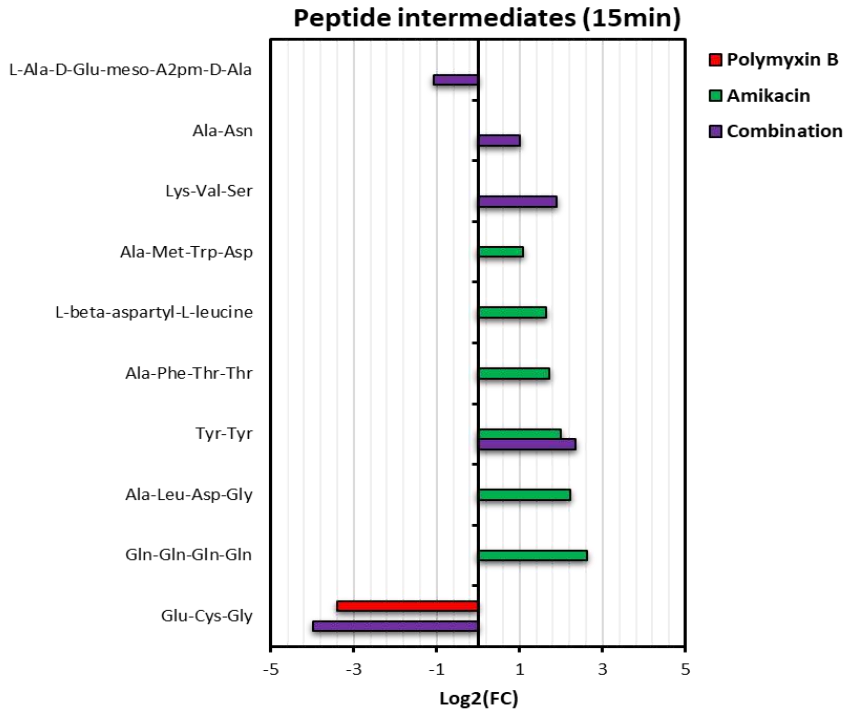

B.

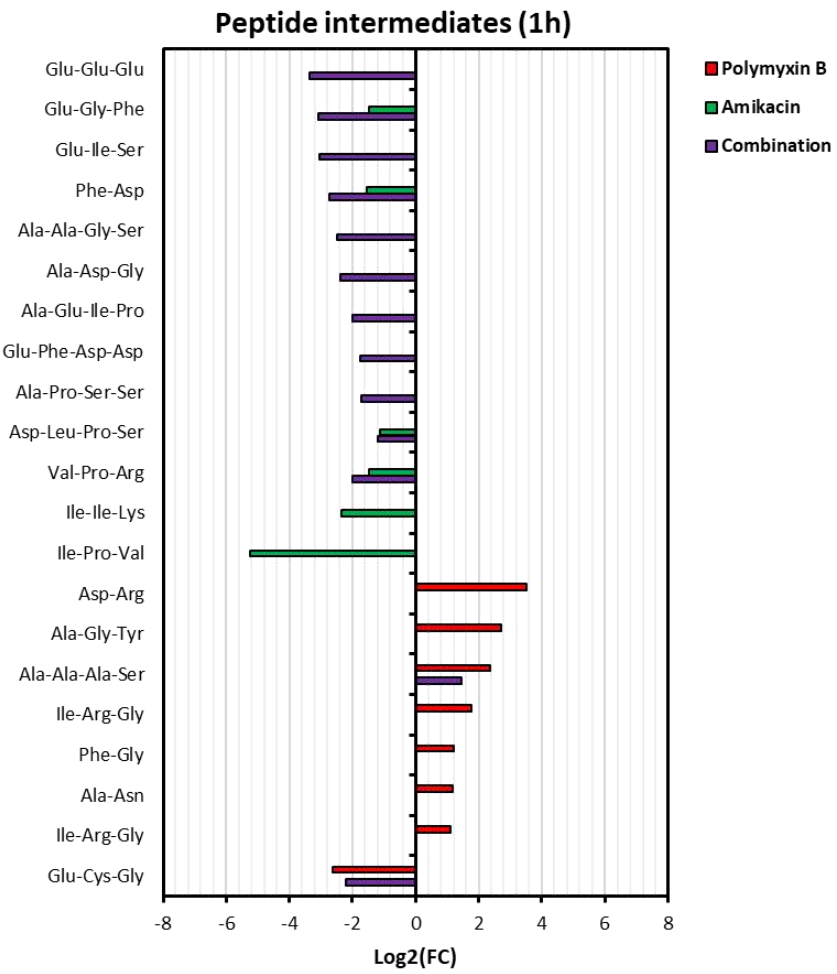

C.